2-Rate Compensation of DC-DC Boost Converter for Wind Turbine Applications

A Thesis

Submitted in partial fulfilment of the requirement for the Degree of

Master in Control System Engineering

(Electrical Engineering Department)

By

Rajdeep Dutta

Registration No.: 163522 of 2022-2023

Examination Roll No.: M4CTL24003

Under the Guidance of

Dr. Sayantan Chakraborty

Department of Electrical Engineering

Jadavpur University, Kolkata-700032, India.

August, 2024

FACULTY OF ENGINEERING AND TECHNOLOGY
JADAVPUR UNIVERSITY

CERTIFICATE

This is to certify that the dissertation entitled **"2-Rate Compensation of DC-DC Boost Converter for Wind Turbine Applications"** has been carried out by RAJDEEP DUTTA (University Registration No.: 163522 of 2022-2023) under my guidance and supervision and be accepted as partial fulfilment of the requirement for the Degree of Master in Control System Engineering. The research results presented in the thesis have not been included in any other paper submitted for the award of any degree to any other University or Institute.

_____

Dr. Sayantan Chakraborty
Thesis Supervisor
Dept. of Electrical Engineering
Jadavpur University

_____

Prof. Biswanath Roy
Head of the Department
Dept. of Electrical Engineering
Jadavpur University

_____

Prof. Dipak Laha
Dean
Faculty of Engineering and Technology
Jadavpur University

FACULTY OF ENGINEERING AND TECHNOLOGY
JADAVPUR UNIVERSITY

CERTIFICATE OF APPROVAL*

The forgoing thesis is hereby approved as a creditable study of an engineering subject and presented in a manner satisfactory to warrant acceptance as prerequisite to the degree for which it has been submitted. It is understood that by this approval the undersigned do not necessarily endorse or approve any statement made, opinion expressed or conclusion drawn there in but approve the thesis only for which it is submitted.

Committee on final examination for the evaluation of the thesis.

_____

Signature of the Examiner

_____

Signature of the Supervisor

*Only in the case the thesis is approved.

FACULTY OF ENGINEERING AND TECHNOLOGY
JADAVPUR UNIVERSITY

DECLARATION OF ORIGINALITY AND COMPLIANCE OF ACADEMIC THESIS

I hereby declare that this thesis entitled **"2-Rate Compensation of DC-DC Boost Converter for Wind Turbine Applications"** contains literature survey and original research work by the undersigned candidate, as part of his Degree of Master in Control System Engineering. All information here have been obtained and presented in accordance with academic rules and ethical conduct. It is hereby declared that, as required by these rules and conduct, all materials and results that are not original to this work have been properly cited and referenced.

Candidate Name: **Rajdeep Dutta**

Examination Roll. No.: M4CTL24003

Thesis Title: **2-Rate Compensation of DC-DC Boost Converter for Wind Turbine Applications**

Date: _____

Place: Signature of the candidate

Acknowledgement

I would like to express my earnest gratitude and sincere thanks to my thesis supervisor Dr. Sayantan Chakraborty, Dept. of Electrical Engineering, Jadavpur University, for giving me the opportunity to work under him and inspiring me to explore the field of Control System Engineering. I am indebted to him for his patient guidance, critical and constructive views and untiring support that shaped my work.

I am also grateful to Prof. Smita Sadhu (Ghosh), Prof. Ranjit Kumar Barai, and Prof Madhubanti Maitra, Department of Electrical Engineering, for all the guidance and knowledge that they have imparted during the tenure of the course.

I would also like to thank my friend and co-worker Siddhartha Chakraborty for his active support and constant encouragement throughout my thesis work.

Lastly, I am thankful to my parents, for their continuous support, encouragement and unending faith in my abilities.

_____

Date:

Rajdeep Dutta

Department of Electrical Engineering

Examination Roll. No.: M4CTL24003

Jadavpur University

Abstract

A boost converter plays a crucial role in wind energy generation systems. The DC-DC boost converter is critical for adapting the variable and often low-voltage output from wind turbines to a stable, higher voltage level suitable for further processing, storage, or grid integration. It plays a key role in maximizing energy capture, improving power quality, and ensuring the efficient operation of wind energy systems. However, the presence of a right-half-plane (RHP) zero is a significant limitation in boost converters, especially in control design and system performance. The right-half-plane zero in a boost converter introduces significant challenges, particularly in terms of control bandwidth, stability, and response time. These limitations affect the overall performance of the boost converter, requiring careful consideration and often complex compensation strategies to mitigate their impact. In this regard, it has been observed in literature that periodic or multi-rate controllers are capable of mitigating the effect of such NMP zeros by means of their loop-zero placement capabilities. This work presents an two-loop control topology that comprises of a PI controller in the inner loop and a generalized 2-rate controller at the outer loop. The robustness as yielded by the 2-rate controller is found to be much better than the PI controller ones. Finally, the proposed methodology is implemented in an Wind Turbine Generating system via MATLAB Simulink environment.

Key words: DC-DC Boost Converter, Wind Turbine, 2-periodic control, 2-rate control.

List of Figures

Figure No.		Page No.
1	A Boost Converter	5
2	Switch On and Diode Off	5
3	Switch Off and Diode On	6
4	Components of a wind turbine	14
5	Types of wind turbine	17
6	Wind Turbine simulation using PMSG and Boost Converter	22
7	Output voltage curve of wind turbine simulation	23
8	A DC-DC boost converter simulink model	25
9	Output voltage response of Fig.8 simulation	25
10	A DC-DC boost converter circuit diagram	26
11	Switch-ON condition	26
12	Switch-OFF condition	27
13	Inductor loop equation model	28
14	Capacitor node equation model	28
15	Small signal equivalent circuit model of boost converter (without DC transformer)	29
16	Small signal equivalent circuit model of boost converter	29
17	Small signal AC equivalent circuit model of boost converter	29
18	Equivalent circuit to find $G_{\hat{v}_{in}}$ after referring primary to secondary side	30
19	Equivalent circuit to find $G_{\hat{d}}$ after referring primary to secondary side	31
20	Double-loop PI structure of a boost converter in continuous time	33
21	Response of double-loop PI compensation of boost converter in continuous time	33
22	Double-loop PI structure of a boost converter in discrete time	34
23(a)	Response of double-loop pi compensation of boost converter in discrete time	34
23(b)	Root Locus for PI compensated outer loop	35
23(c)	Zoomed-in portion of the Root Locus of Fig. 23(b)	35
24	Simscape model of double-loop PI compensation of boost converter	36
25	Response of Simscape model of double-loop pi compensation of boost converter	36
26	The 2-Periodic controller in 1-DOF form and the LTI plant	39
27	Fast-output controller scheme	50
28	Fast-input controller scheme	51
29	A Generalised m-th order 2-rate controller	52
30	MATLAB Simulink implementation of 2-rate control	54
31	Output response curve of Fig.30 simulation	54
32	Root Locus of the system compensated by Multi (2)-rate control	55
33	Augmentation Block Diagram	57
34	Root locus for 2-rate compensated plant	58
35	Double-loop control of boost converter with 2-rate control in outer loop	62
36	Output response curve for the 2-rate compensated system	62
37	The subsystem model of 2-rate control shown in Fig.35	63
38	Simulink model of Wind turbine and boost converter with 2-rate compensation	64
39	Wind Turbine Subsystem	64
40	Output response curve for double-loop compensation of boost converter for wind power generation	65

List of Tables

Table No.		Page No.
1	Function and description of different components of a wind turbine	14

List of abbreviations

NMP	:	Non-Minimum-Phase
CL	:	Closed Loop
RL	:	Root Locus
Eqn.	:	Equation
LTI	:	Linear Time Invariant
PWM	:	Pulse Width Modulation
DOF	:	Degrees-of-Freedom
DC	:	Direct Current
AC	:	Alternating Current
MPPT	:	Maximum Power Point Tracking
SISO	:	Single Input Single Output
GM	:	Gain Margin

TABLE OF CONTENTS

Chapter 1: Introduction and Literature Review **1**

1.1 Introduction 1

1.2 Wind energy and wind turbine 3

1.3 Boost Converter 4

1.4 Motivation 12

1.5 Thesis Organization 12

Chapter 2: Wind Turbine: Mathematical Modelling and MATLAB Simulation **13**

2.1 Wind Turbine 13

2.2 Mathematical Modelling of Wind Turbine 18

2.3 Wind Turbine Simulation using PMSG and Boost Converter 22

Chapter 3: Small Signal AC Equivalent Model and Double-Loop PI-compensation of Boost Converter **24**

3.1 MATLAB simulation of Boost Converter 24

3.2 Small signal AC model of a Boost Converter 26

3.3 PI Compensation of Boost Converter 30

Chapter 4: Multi/2-Rate Control From a 2-Periodic Perspective: A Review **38**

4.1 Limitation of LTI controllers 38

4.2 2-Periodic controller 39

4.3 Multi-Rate Control 49

4.4 Multi (2)-Rate Control from a 2-Periodic Perspective: Generalized 2-Rate Control 52

Chapter 5: Implementation of 2-Rate Control for Boost Converter **56**

5.1 Augmentation of boost converter 56

5.2 Controller Synthesis 57

5.3 Conclusion 65

Chapter 6: Conclusion and Future Scope **66**

6.1 Conclusion 66

6.2 Future Scope 66

References 68

Chapter 1

Introduction and Literature Review

1.1 Introduction:

Wind energy has emerged as one of the most promising renewable energy sources, offering a sustainable and eco-friendly alternative to fossil fuels. The integration of wind energy into the electrical grid, however, presents several technical challenges. One key challenge is the variability and intermittency of wind, which leads to fluctuating output voltages from wind turbines. To address this issue, DC-DC boost converters play a crucial role in stabilizing and optimizing the voltage levels, enabling efficient power transfer from wind turbines to the grid or energy storage systems.

1.1.1 Wind Energy Conversion Systems

A typical wind energy conversion system consists of the following components:

1. **Wind Turbine**: Converts kinetic energy from the wind into mechanical energy.
2. **Generator**: Converts mechanical energy from the turbine into electrical energy, typically producing variable AC or DC output depending on the generator type.
3. **Power Electronic Converter**: Includes DC-DC converters, which regulate the voltage and ensure compatibility with the grid or energy storage systems [35].

4. **Control System**: Manages the operation of the turbine and converter, often incorporating MPPT to maximize energy extraction [35].

1.1.2 DC-DC Boost Converters

A DC-DC boost converter is an electronic device that steps up (boosts) a lower input DC voltage to a higher output DC voltage. It operates based on the principle of energy storage in inductors and capacitors, using switching elements like transistors to control the energy transfer. The main components of a boost converter include:

- **Inductor**: Stores energy when the switch is on and releases it when the switch is off.
- **Capacitor**: Smoothens the output voltage.
- **Diode**: Prevents the capacitor from discharging back into the circuit.
- **Switch (usually a MOSFET)**: Controls the charging and discharging of the inductor.

1.1.3 Role of Boost Converters in Wind Energy Applications

1. **Voltage Regulation**: Wind turbines generate a variable output voltage due to fluctuating wind speeds. The DC-DC boost converter steps up this variable voltage to a consistent, higher voltage level suitable for grid connection or battery charging [35]. This ensures a stable power supply regardless of changes in wind conditions.
2. **Maximum Power Point Tracking (MPPT)**: To maximize the efficiency of wind energy conversion, it's essential to operate the wind turbine at its optimal power point. The DC-DC boost converter, in combination with MPPT algorithms, adjusts the turbine's operating point by varying the duty cycle of the converter. This dynamic adjustment ensures that the maximum possible energy is harvested from the wind [35].
3. **Grid Integration**: For wind energy systems that are connected to the electrical grid, it is crucial to match the voltage levels with those of the grid. A DC-DC boost converter can step up the turbine's output to match the grid's requirements, ensuring seamless integration and efficient power transfer [36].
4. **Battery Charging**: In off-grid wind energy systems or hybrid systems with energy storage, the generated power needs to be stored in batteries. Since batteries require a specific charging voltage, a DC-DC boost converter can adjust the turbine's output to the appropriate voltage level for efficient battery charging, thereby enhancing the overall system reliability.

5. **Enhancing System Efficiency**: By optimizing the voltage levels and ensuring that the wind turbine operates close to its maximum power point, DC-DC boost converters contribute to the overall efficiency of the wind energy system [35]. This leads to better energy yield and a lower cost per kilowatt-hour of electricity generated.

1.2 Wind energy and wind turbine:

Wind energy, a prominent renewable energy source, converts the kinetic energy of wind into electricity, offering a sustainable alternative to fossil fuels. The process by which air masses move across the Earth's surface due to uneven solar heating is well-established in the literature. Wind turbines are the primary technology used to capture this kinetic energy and convert it into mechanical and electrical energy [1].

1.2.1 Wind Energy

The environmental benefits of wind energy are extensively documented. Unlike fossil fuels, wind energy production does not result in greenhouse gas emissions or water contamination, making it a clean energy source as described in [2]. Additionally, the reliance on finite resources like coal and natural gas is reduced, enhancing energy security [3]. The economic advantages are also significant; after installation, wind farms incur relatively low operational costs, and they stimulate job creation in various sectors, including manufacturing, installation, and maintenance [4].

Nevertheless, wind energy presents certain challenges. Wind speed variability, which leads to intermittent power generation, necessitates backup systems or energy storage solutions to maintain a stable electricity supply [5]. Furthermore, the ecological impacts of wind turbine installation, such as bird and bat mortality and noise pollution, require careful site selection and technological advances to mitigate [6].

1.2.2 Wind Turbines

Wind turbines are central to converting wind energy into electricity. These systems typically include rotor blades, a nacelle, a gearbox, a generator, and a tower. The rotor blades capture

wind energy and convert it into rotational motion, which is subsequently transformed into electricity by the generator [7]. Advances in wind turbine design, materials, and control systems have greatly improved their efficiency, leading to taller turbines with longer blades that capture

more energy [8]. Innovations in control systems have optimized turbine operations across varying wind conditions, as mentioned in [9].

Two main types of wind turbines are highlighted in the literature: horizontal-axis wind turbines (HAWTs) and vertical-axis wind turbines (VAWTs). HAWTs, which are more widely used due to their higher efficiency, have their rotor axis parallel to the ground. Conversely, VAWTs, which have a perpendicular rotor axis, are beneficial in specific scenarios, such as areas with turbulent wind or space constraints [10].

Wind turbines can be installed onshore or offshore. Onshore wind farms are more common due to lower installation costs, while offshore wind farms benefit from stronger, more consistent winds, leading to higher energy output. However, offshore installations are more complex and costly, requiring advanced technology and maintenance practices to ensure efficiency, as discussed.

In summary, wind energy and wind turbines represent a promising solution for sustainable energy production. Despite challenges such as variability and ecological impact, ongoing advancements in technology continue to improve the efficiency and reliability of wind energy systems, paving the way for a more sustainable energy future.

1.3 Boost Converter:

A boost converter, also known as a step-up converter, is a type of DC-DC converter that increases (or "boosts") the input voltage to a higher output voltage. DC-DC boost converters are integral to the efficient operation of wind energy systems. It plays a key role in voltage stabilization, MPPT, grid compatibility, and energy storage integration [35]. By optimizing the voltage levels and ensuring that wind turbines operate at their maximum efficiency, boost converters contribute to the overall effectiveness and reliability of wind energy systems.

1.3.1 Operating Principle

The basic operation of a boost converter is relatively straightforward. It consists of four main components: an inductor, a switch (usually a transistor), a diode, and a capacitor. The operation can be divided into two primary modes:

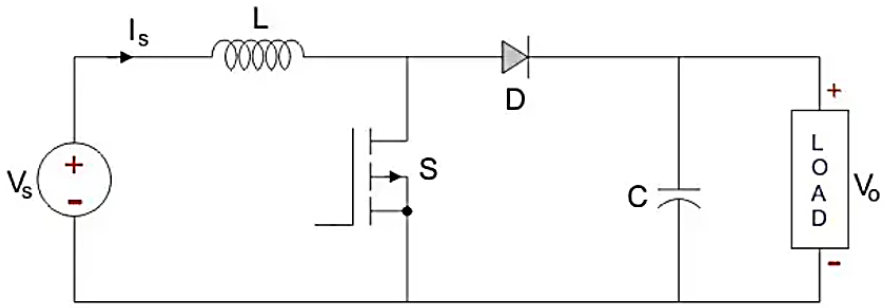

Fig.1: A Boost Converter [11]

1. Switch On Mode:

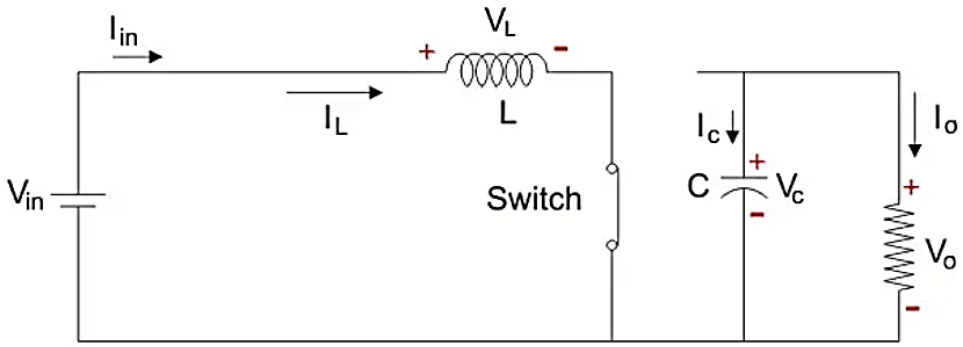

Fig.2: Switch On and Diode Off [11]

When the switch is closed (turned on), the input voltage is applied across the inductor. This causes the inductor to store energy in the form of a magnetic field. During this time, the diode is reverse-biased, preventing current from flowing to the output [37].

Let us say the switch is on for a time T_{ON} and is off for a time T_{OFF}. We define the time period, T, as $T = T_{ON} + T_{OFF}$.

Let us now define another term, the duty cycle, $D = \frac{T_{ON}}{T}$

Using KVL in the inductor loop:

$$V_{in} = V_L = L\frac{di_L}{dt} \tag{1.1}$$

$$\Rightarrow \frac{di_L}{dt} = \frac{\Delta i_L}{\Delta t} = \frac{\Delta i_L}{DT} = \frac{V_{in}}{L} \tag{1.2}$$

Since the switch is closed for a time $T_{ON} = DT$ we can say that $\Delta t = DT$.

$$\therefore (\Delta i_L)_{closed} = \left(\frac{V_{in}}{L}\right) DT \tag{1.3}$$

While performing the analysis of the Boost converter, we have to keep in mind that the inductor current is continuous and this is made possible by selecting an appropriate value of L. The inductor current in steady state rises from a value with a positive slope to a maximum value during the ON state and then drops back down to the initial value with a negative slope [11]. Therefore, the net change of the inductor current over anyone complete cycle is zero.

2. Switch Off Mode:

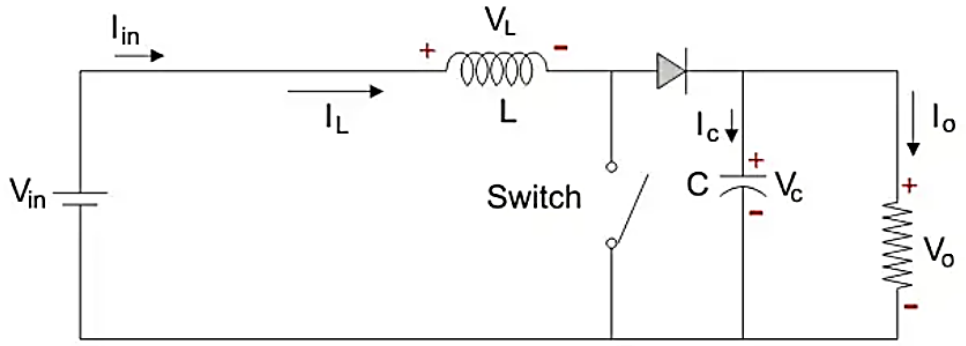

Fig.3: Switch Off and Diode On [11]

Since, the switch is open for a time $T_{OFF} = T - T_{ON} = T - DT = (1 - D)T$

We can say that $\Delta t = (1 - D)T$

In this mode using KVL we get:

$$(\Delta i_L)_{open} = \left(\frac{V_o - V_{in}}{L}\right)(1 - D)T \tag{1.4}$$

It is already established that the net change of the inductor current over any one complete cycle is zero.

$$\therefore (\Delta i_L)_{closed} + (\Delta i_L)_{open} = 0 \tag{1.5}$$

$$=> \frac{V_o}{V_{in}} = \frac{1}{1-D} \tag{1.6}$$

The duty cycle (D) varies between 0 and 1.

1.3.2 Application of Boost Converter

Boost converters are used in a wide range of applications:

- **Battery-Powered Devices:** To step up the voltage from a battery to a higher level required by the device circuitry.

- **Renewable Energy Systems:** In photovoltaic (solar) systems, boost converters are used to step up the low voltage output from solar panels to a higher voltage for grid-tie inverters or battery charging [35].
- **Power Supply Systems:** In systems where the input voltage may drop below the required operating level, a boost converter can maintain a stable output voltage [12,13].

1.3.3 Challenges and Design Considerations

Designing a boost converter involves several challenges, including managing the non-minimum phase behaviour, selecting appropriate components, and ensuring stability under varying load conditions.

- **Non-Minimum Phase Behaviour:** The boost converter exhibits a right-half-plane zero in its transfer function, which can complicate control design. Advanced control strategies are often employed to manage this issue.
- **Component Selection:** The inductor size, switch rating, and diode selection must be carefully chosen to handle the desired power levels while minimizing losses.
- **Stability and Transient Response:** Ensuring a fast transient response and maintaining stability under load changes are crucial, particularly in dynamic applications like power supplies for portable electronics [14,15,16].

The boost converter is a versatile and widely used power conversion device that plays a critical role in many modern electronic systems. Its ability to efficiently step up voltage levels makes it indispensable in applications ranging from consumer electronics to renewable energy systems. Ongoing advancements in control techniques and component technologies continue to enhance the performance and efficiency of boost converters, enabling their use in increasingly demanding applications.

1.3.4 Control Strategies implemented for DC-DC boost Converters

Implementing a control strategy in a DC-DC boost converter is crucial to ensure optimal performance, efficiency, and stability of the system. The control strategy primarily focuses on regulating the output voltage, maintaining a constant output despite variations in the input voltage or load, and maximizing the efficiency of the conversion process. Below is an overview of the key aspects of implementing a control strategy in a DC-DC boost converter:

1.3.5 The Control Objectives

The main objectives of a control strategy in a DC-DC boost converter are:

- **Output Voltage Regulation**: Maintain a stable output voltage regardless of changes in input voltage or load conditions.
- **Efficiency Optimization**: Minimize energy losses during conversion.
- **Dynamic Response**: Quickly respond to changes in input or load to minimize transients.
- **Protection**: Prevent over-voltage, over-current, and other fault conditions [38].

Different control strategies offer various advantages depending on the specific application and performance requirements. Below are some of the key control strategies commonly used in DC-DC boost converters:

Voltage-mode control is a widely used control strategy where the output voltage is regulated by comparing it to a reference voltage. The error between the reference and the actual output voltage is processed by a compensator, usually a Proportional-Integral-Derivative (PID) controller, which adjusts the duty cycle of the switch to maintain the desired output voltage[39].

- **Pros**:
    - Simple to implement.
    - Well-suited for applications with relatively stable input voltage and load conditions.
- **Cons**:
    - May have slower dynamic response compared to current-mode control.
    - Less effective in handling large variations in input voltage.

Current-mode control adds an inner current loop to the voltage loop. This strategy regulates the inductor current directly, in addition to the output voltage. The inner loop controls the inductor current by adjusting the duty cycle based on the error between the measured current and a reference current. The outer voltage loop adjusts the reference current to maintain the desired output voltage.

- **Pros**:
    - Improved dynamic response and stability.

    - Inherent over-current protection.
    - Better performance under varying input voltage and load conditions.
- **Cons**:
    - More complex to implement due to the need for current sensing.
    - Potential for subharmonic oscillation in continuous conduction mode (CCM), requiring slope compensation.

Hysteretic control, also known as bang-bang control, directly regulates the output voltage by turning the switch on or off based on whether the output voltage is above or below certain thresholds [38]. This approach is known for its simplicity and fast dynamic response.

- **Pros**:
    - Extremely simple to implement.
    - Fast response to changes in load or input voltage.
- **Cons**:
    - Results in variable switching frequency, which can complicate filter design and EMI management.
    - Less precise control compared to other strategies.

Sliding mode control is a non-linear control method that forces the system to operate on a predefined sliding surface, regardless of disturbances or parameter variations. It is robust and capable of handling large variations in input and load.

- **Pros**:
    - Robust to parameter variations and external disturbances.
    - Good dynamic performance and fast response.
- **Cons**:
    - Complex to design and implement.
    - Potential for chattering (rapid switching), which can cause wear on components and generate EMI.

Average current mode control is a variation of current-mode control where the control loop regulates the average value of the inductor current, rather than its peak value. This method provides smoother operation and can be more stable than peak current-mode control [39].

- **Pros**:
    - Smooth and stable operation.
    - Good performance in both continuous and discontinuous conduction modes.
- **Cons**:
    - Requires more complex control circuitry and accurate current sensing.

Digital control involves using a microcontroller or digital signal processor (DSP) to implement the control strategy. It allows for more sophisticated algorithms, such as adaptive control, predictive control, or even machine learning-based control.

- **Pros**:
    - Flexibility to implement complex control algorithms.
    - Easier to integrate with digital systems and communication protocols.
    - Ability to implement adaptive control that adjusts parameters in real-time.
- **Cons**:
    - Requires analog-to-digital conversion, which introduces sampling delay and potential quantization errors.
    - Higher cost and complexity compared to analog control.

Proportional-Integral-Derivative (PID) control is a classic control strategy that combines three terms: proportional, integral, and derivative. The proportional term responds to the current error, the integral term accounts for past errors, and the derivative term predicts future errors. This combination provides a balance of speed, stability, and accuracy [39].

- **Pros**:
    - Widely used and well-understood.
    - Good balance between response speed and stability.
- **Cons**:
    - Requires tuning of three parameters (P, I, D), which can be complex in some systems.
    - May not perform well in highly non-linear systems without additional adjustments.

Fuzzy logic control is a non-linear control method that mimics human decision-making. It uses a set of fuzzy rules to handle imprecise inputs and provides smooth control actions. This method is particularly useful in systems with a high degree of uncertainty or non-linearity.

- **Pros**:
    - Handles non-linearities and uncertainties well.
    - No need for precise mathematical modelling.
- **Cons**:
    - Requires expert knowledge to define fuzzy rules.
    - Computationally intensive, particularly for real-time applications.

Predictive control anticipates future system behaviour based on a model of the converter and adjusts the control inputs to optimize performance. This method is effective in systems where the dynamics are well understood and can be predicted accurately.

- **Pros**:
    - Optimizes control actions based on future predictions.
    - Can improve efficiency and response time.
- **Cons**:
    - Requires a precise model of the system.
    - Computationally demanding, especially for real-time applications.

Implementing a control strategy in a DC-DC boost converter is a critical step in achieving reliable and efficient performance. Choosing the right control strategy for a DC-DC boost converter depends on the specific requirements of the application, including the desired performance, complexity, and cost constraints. Voltage-mode and current-mode controls are the most commonly used, offering a good balance between simplicity and performance. For applications requiring fast response or robustness to disturbances, advanced techniques like sliding mode, digital control, or predictive control may be more appropriate [39]. Proper design, implementation, and tuning of these control strategies are essential to achieving optimal performance in DC-DC boost converters. Advanced strategies, such as digital control and sliding mode control, offer additional robustness and flexibility, making them suitable for modern, high-performance applications.

1.4 Motivation

It is important to recognize that boost converters contain NMP zeros. LTI systems that include both unstable poles and NMP zeros typically suffer from poor stability margins when controlled using LTI controllers. However, multi-rate control strategies have been shown to address the limitations of LTI controllers effectively. Therefore, employing multi-rate control in boost converter systems presents a promising solution. Boost converters are utilized in wind turbines to step up the low voltage generated by the turbine to a higher voltage required for efficient energy transfer and grid integration. This study explores the application multi-rate controllers for the compensation of boost converters, which are commonly used in wind turbine systems.

1.5 Thesis Organization

Chapter 1 explores about wind energy, wind turbine and also boost converter. The operating principle of boost converter is discussed here. Finally, it discusses the motivation behind this thesis.

Chapter 2 describes the wind turbine in detail stating its working principle, components, advantages, challenges and its mathematical modelling. Then a MATLAB simulation is provided showing the working of a boost converter with the wind turbine as its input.

Chapter 3 includes simulation of a boost converter using PWM. Then the small signal model of a boost converter is discussed. A key aspect of this thesis – two-loop PI compensation of boost converter is analysed.

Chapter 4 revisits a 1-DOF 2-periodic controller configuration along with multi-rate control. Also a generalised 2-rate controller is discussed along with an example.

Chapter 5 shows use of generalised 2-rate control for a boost converter in a two-loop configuration with wind turbine as the reference source of input energy.

Chapter 2

Wind Turbine: Mathematical Modelling and MATLAB Simulation

2.1 Wind Turbine:

Wind turbines are sophisticated devices that convert the kinetic energy of wind into electrical energy. They play a crucial role in the global shift towards renewable energy sources, offering a sustainable alternative to fossil fuels. Despite some challenges, ongoing technological advancements are making wind energy more efficient and cost-effective, ensuring it will play a central role in the future energy landscape.

2.1.1 Working Principle:

A wind turbine turns wind energy into electricity using the aerodynamic force from the rotor blades, which work like an airplane wing or helicopter rotor blade. When wind flows across the blade, the air pressure on one side of the blade decreases. The difference in air pressure across the two sides of the blade creates both lift and drag. The force of the lift is stronger than the drag and this causes the rotor to spin. The rotor connects to the generator, either directly (if it's a direct drive turbine) or through a shaft and a series of gears (a gearbox) that speed up the rotation and allow for a physically smaller generator. This translation of aerodynamic force to rotation of a generator creates electricity [26,29].

2.1.2 Components:

A typical wind turbine consists of several key components, each serving a distinct function:

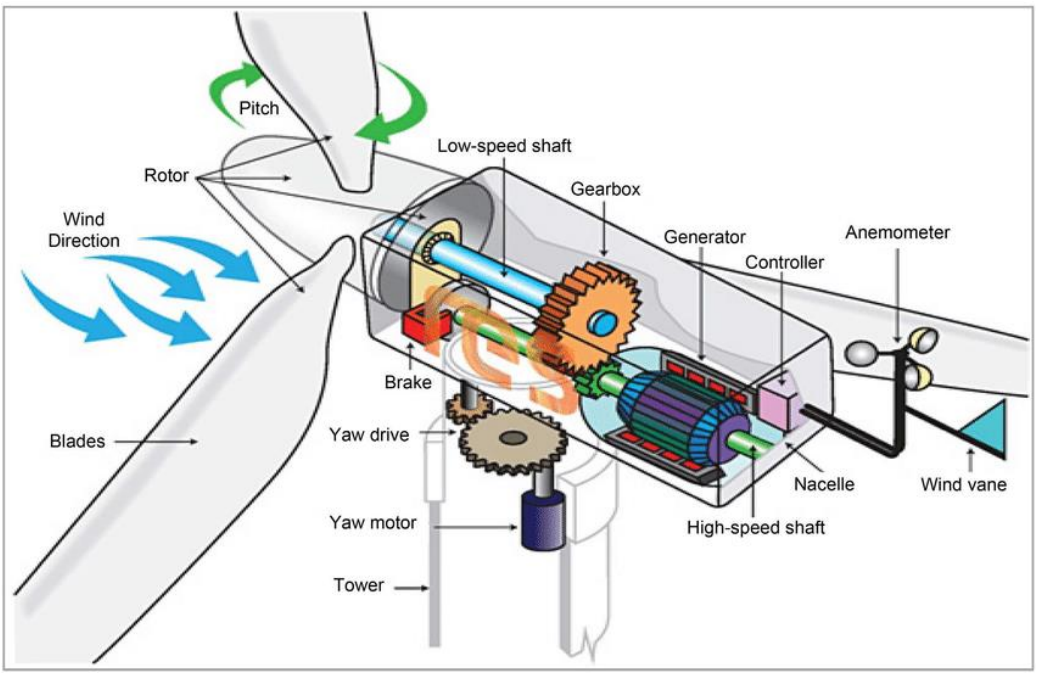

Fig.4: Components of a wind turbine[30]

Table 1: Function and description of different components of a wind turbine

Component Name	Function	Description
Blades	Capture the wind's energy.	Aerodynamically shaped to maximize lift and minimize drag. The most common configuration is three blades.
Rotor	Converts wind energy into rotational energy.	Includes the blades and the hub. When the wind blows, it causes the rotor to spin.
Pitch:	Controls the angle of the blades.	Adjusts the blade angle to control the rotational speed and optimize efficiency, especially during high winds to prevent damage.

Low-speed Shaft	Transfers the rotational energy from the rotor to the gearbox.	Connects the rotor to the gearbox, rotating at the same low speed as the rotor.
Gearbox	Increases the rotational speed.	Steps up the speed from the low-speed shaft to the high-speed shaft, which is necessary for efficient electricity generation.
Brake	Stops the rotor in emergency conditions.	Ensures the turbine can be safely stopped for maintenance or during extreme wind conditions.
Yaw Drive	Rotates the nacelle to face the wind.	Ensures the rotor is optimally aligned with the wind direction.
Yaw Motor	Powers the yaw drive.	An electric motor that drives the yaw system to rotate the nacelle.
Tower	Elevates the turbine components.	Supports the nacelle and rotor blades at a height where wind speeds are higher and more consistent.
Nacelle	Houses critical components	Contains the gearbox, generator, and other essential parts, protecting them from the environment.

Generator	Converts mechanical energy into electrical energy.	Uses electromagnetic induction to generate electricity from the rotational energy provided by the high-speed shaft.
Controller	Manages the operation of the turbine.	Monitors the turbine's status and controls its operation, including start-up, shut-down, and optimization.
High-speed Shaft	Transfers energy from the gearbox to the generator.	Rotates at a higher speed than the low-speed shaft, suitable for efficient generator operation.
Anemometer	Measures wind speed.	Provides data to the controller to optimize the turbine's operation based on wind conditions.
Wind Vane	Measures wind direction.	Helps the yaw drive and yaw motor to correctly orient the nacelle and rotor towards the wind.

2.1.3 Types of Wind Turbines:

1. **Horizontal Axis Wind Turbines (HAWTs)**: These are the most common type, with the main rotor shaft and electrical generator at the top of a tower. They must be pointed into the wind to function efficiently.

2. **Vertical Axis Wind Turbines (VAWTs)**: These have the main rotor shaft arranged vertically. VAWTs do not need to be pointed into the wind, making them suitable for locations where wind direction is variable [28].

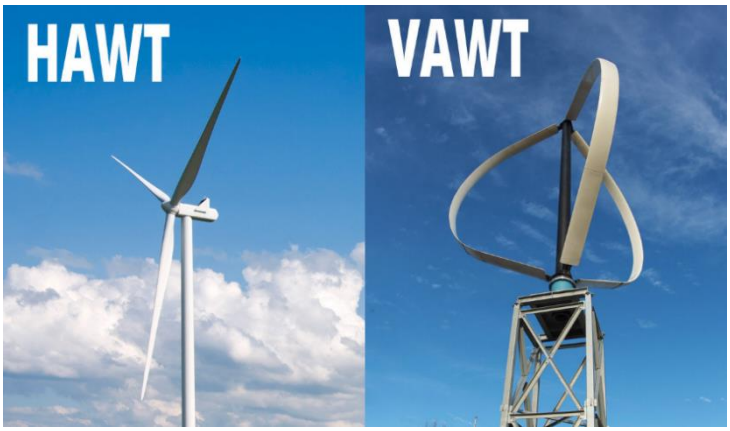

Fig.5: Types of wind turbine

2.1.4 Advantages and Challenges:

Advantages:

- **Renewable Energy Source**: Wind energy is abundant, inexhaustible, and available in many parts of the world.
- **Low Operational Costs**: Once installed, wind turbines have relatively low maintenance and operation costs.
- **Environmental Benefits**: Wind turbines produce no emissions during operation, significantly reducing the carbon footprint compared to fossil fuel-based power plants.

Challenges:

- **Intermittency**: Wind is not always constant, and energy production can be unpredictable.
- **Initial Costs**: The initial investment for wind turbine installation can be high.
- **Aesthetic and Environmental Impact**: Some people find wind turbines visually unappealing, and they can have impacts on local wildlife, particularly birds and bats.

2.2 Mathematical Modelling of Wind Turbine:

Mathematical modelling of wind turbines involves deriving the equations that describe the physical behaviour and performance of the turbine under various wind conditions [25]. The model includes the aerodynamics of the rotor, the mechanics of the drive train, the dynamics of the generator, and the control systems.

2.2.1 Aerodynamics of the Rotor:

- The power extracted by the wind turbine from the wind is given by the power equation:

$$P_{turbine} = \frac{1}{2}\rho A v^3 C_p(\lambda, \beta) \quad (2.1)$$

where:

- $P_{turbine}$ is the power extracted by the turbine (W)
- ρ is the air density (kg/m³), the density of the air affects how much kinetic energy is in the wind. Higher density means more energy
- A is the swept area of the rotor (m²), the area through which the wind passes. Larger area means more wind is captured
- v is the wind speed (m/s), since power is proportional to the cube of the wind speed, small increases in wind speed lead to large increases in power.
- $C_p(\lambda, \beta)$ is the power coefficient, which is a function of the tip-speed ratio λ and the pitch angle β.

Derivation:

The kinetic energy (E) of an object with mass (m) and velocity (v) is given by:

$$E = \frac{1}{2}mv^2 \quad (2.2)$$

For a stream of air with a mass flow rate ($\dot{m}$) and velocity (v), the kinetic energy per second (power) is:

$$P_{wind} = \frac{1}{2}\dot{m}v^2 \quad (2.3)$$

The mass flow rate ($\dot{m}$) of the air passing through the rotor swept area (A) is:

$$\dot{m} = \rho A v \quad (2.4)$$

where:

- ρ is the air density (kg/m³),
- A is the swept area of the rotor ($A = \pi R^2$ where R is the radius of the rotor),
- v is the wind speed (m/s).

Substituting the mass flow rate into the kinetic energy equation gives:

$$P_{wind} = \frac{1}{2}\rho A v^3 \quad (2.5)$$

This equation represents the total power available in the wind. However, not all this power can be captured by the wind turbine.

The power extracted by the turbine ($P_{turbine}$) is a fraction of the total power in the wind, determined by the power coefficient (C_p):

$$P_{turbine} = \frac{1}{2}\rho A v^3 C_p \quad (2.6)$$

The power coefficient (C_p) is a dimensionless factor that is typically determined through experimental data or complex numerical simulations. It represents the efficiency of the turbine in converting the kinetic energy of the wind into mechanical energy. It is a function of the tip-speed ratio (λ) and the blade pitch angle (β):

$$C_p = f(\lambda, \beta) \quad (2.7)$$

The tip-speed ratio λ is defined as [25]:

$$\lambda = \frac{\text{blade tip speed}}{\text{wind speed}} = \frac{\omega R}{v} \quad (2.8)$$

where:

- ω is the rotational speed of the rotor (rad/s),
- R is the radius of the rotor (m).

Combining these steps, the power extracted by the wind turbine from the wind is given by:

$$P_{turbine} = \frac{1}{2}\rho A v^3 C_p(\lambda, \beta) \quad (2.9)$$

2.2.2 Mechanics of the Drive Train

The drive train model links the rotor to the generator. The rotational dynamics of the rotor are described by:

$$J_r\left(\frac{d\omega}{dt}\right) = T_r - T_g - D_r\omega \quad (2.10)$$

where:

- J_r is the moment of inertia of the rotor (kg·m²),
- $\frac{d\omega}{dt}$ is the angular acceleration of the rotor (rad/s²),
- T_r is the aerodynamic torque produced by the rotor (N·m),
- T_g is the generator torque (N·m),
- D_r is the damping coefficient of the rotor (N·m·s).

The aerodynamic torque T_r can be expressed as:

$$T_r = \frac{P}{\omega} = \frac{1}{2}\rho A v^3 \frac{C_p(\lambda,\beta)}{\omega} \quad (2.11)$$

2.2.3 Dynamics of the Generator:

The electrical power generated by the generator P_g is given by:

$$P_g = \eta_g T_g \omega \quad (2.12)$$

where: η_g is the efficiency of the generator.

The dynamics of the generator can be modelled using the generator's electrical characteristics and control system. For a simplified model, we can assume a linear relationship between the generator torque T_g and the electrical power output.

2.2.4 Control Strategies:

Wind turbines use control systems to optimize performance and ensure safety. Two common control mechanisms are:

- **Pitch Control**: Adjusts the blade pitch angle β to regulate the power output and rotor speed. The control objective is to maintain optimal C_p and protect the turbine from excessive wind speeds.
- **Torque Control**: Adjusts the generator torque T_g to control the rotor speed ω. This can be done using feedback loops to maintain the desired tip-speed ratio λ.

The control algorithms are often implemented using PID (Proportional-Integral-Derivative) controllers, with set points derived from the desired operating conditions of the turbine.

2.2.5 Coupled System Equations:

Combining the above models, the overall system of equations describing the wind turbine dynamics is [25]:

- Aerodynamic power: $P_{turbine} = \frac{1}{2}\rho A v^3 C_p(\lambda, \beta)$
- Tip-speed ratio: $\lambda = \frac{\omega R}{v}$
- Rotor dynamics: $J_r\left(\frac{d\omega}{dt}\right) = \frac{1}{2}\rho A v^3 \frac{C_p(\lambda,\beta)}{\omega} - T_g - D_r\omega$
- Generator power: $P_g = \eta_g T_g \omega$
- Control laws: $\beta = f(v, \omega, P)$ and $T_g = g(v, \omega, P)$,

where f and g represent the control algorithms for pitch and torque control respectively.

2.3 Wind Turbine simulation using PMSG and Boost Converter:

A wind turbine converts kinetic energy from wind into mechanical energy as the rotor blades spin. This mechanical energy rotates the shaft of a Permanent Magnet Synchronous Generator (PMSG), which then generates alternating current (AC) electrical energy through electromagnetic induction. The generated AC voltage is rectified to direct current (DC) and fed into a boost converter, which steps up the DC voltage to a higher, more stable level suitable for grid integration or other applications.

The system is implemented using MATLAB Simulink with the following set of values:

- Pitch angle = 0°
- Wind speed = 12m/s
- Generator power(P_g)=12.3KW
- Tip-speed ratio: $\lambda = 8.1$
- Radius of rotor (R) = 1.3m
- Rated generator speed (ω)= $\frac{\lambda \text{ x wind speed}}{R} = \frac{8.1*12}{1.3} = 74.769 \frac{rad}{s}$
- Capacitance at input of boost converter (C1) = 450e-6 F
- Inductor(L)= 8e-3 H
- Boost converter capacitance (C)= 8e-6 F
- Resistance(R)=200Ω
- Duty ratio(D)=0.5

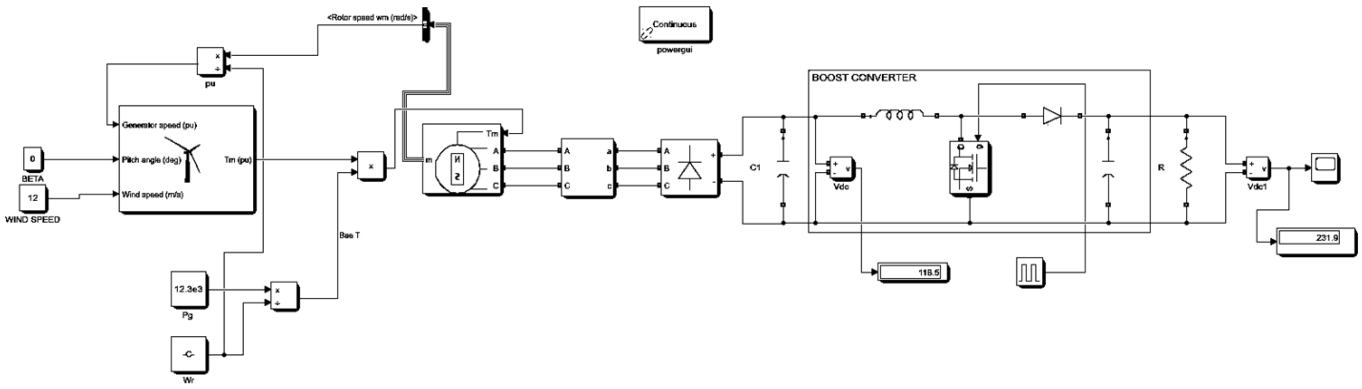

Fig.6: Wind Turbine simulation using PMSG and Boost Converter

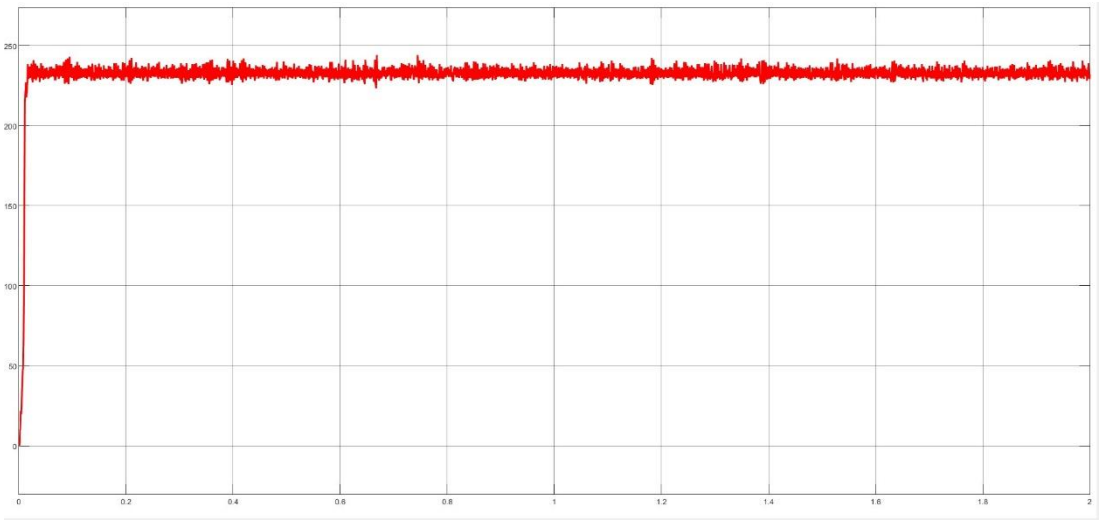

Fig.7: Output voltage curve of wind turbine simulation

For an input of 118.5V to the boost converter we are getting 231.9V. Ideally for D=0.5 the output should have been 237V, hence an offset is observed in the obtained value, which can be further compensated by using suitable controller.

Chapter 3

Small Signal AC Equivalent Model and Double-Loop PI-compensation of Boost Converter

3.1 MATLAB simulation of Boost Converter:

A brief overview and the description of DC-DC Boost converter is discussed in Section 1.3.1. This section presents a simulation of a DC-DC Boost converter circuit using MATLAB Simulink platform.

A boost converter steps up the input DC voltage to a higher output voltage by storing energy in an inductor during the "on" phase of a switch and releasing it through a diode and capacitor during the "off" phase. The output voltage V_{out} is given by the equation:

$$V_{out} = \frac{V_{in}}{1 - D} \quad (as\ derived\ in\ eqn\ (1.6))$$

where V_{in} is the input voltage and D is the duty cycle (the fraction of time the switch is "on"). As D increases, the output voltage increases.

In MATLAB Simulink a boost converter is implemented, using specific component values for the inductor, capacitor, and load resistance. The pulse generator provided the control signal to the switch, defining the duty cycle for the converter.

The parameters values considered for simulation are as follows:

- Input DC voltage(V_{in}) = 15V

- Inductor(L)=8mH
- Capacitor(C)=8μF
- Resistor(R)=200Ω
- Duty ratio(D)=0.5 i.e. 50% hence, $\acute{D}$= (1-D) = 0.5

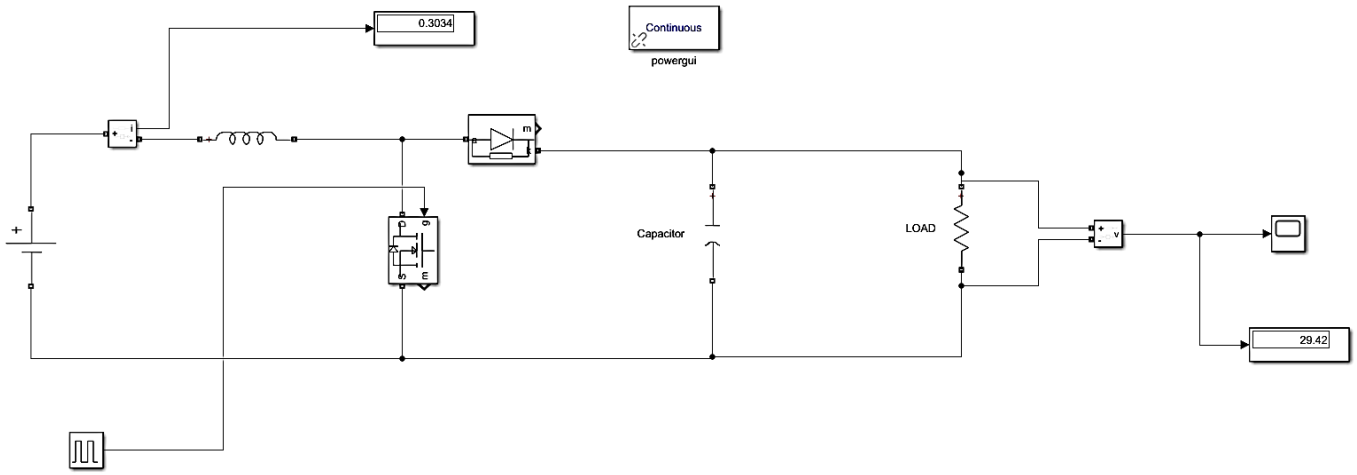

Fig.8: A DC-DC boost converter simulink model

So, here we can see that 15V DC voltage is steeped up into 29.42V due to given duty ratio of 0.5. Ideally it should had been 30V, hence here also an offset is observed, which we can compensate by use of controller. The output voltage response is shown in Figure 9.

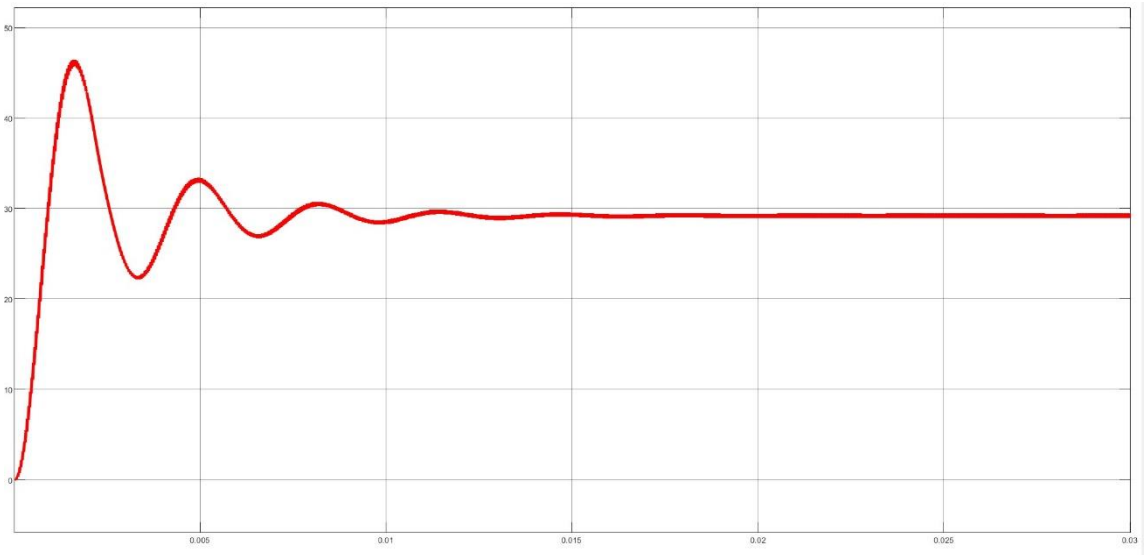

Fig.9: Output voltage response of Fig.8 simulation

3.2 Small signal AC model of a Boost Converter:

A boost converter circuit is considered with symbols having usual meanings:

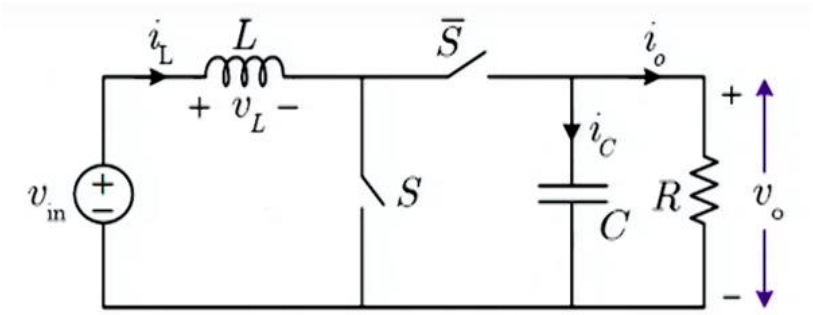

Fig.10: A DC-DC boost converter circuit diagram

Now, there can be two conditions with S-ON and S-OFF. Analysing that two conditions:

1. With S-ON and $\bar{S}$-OFF:

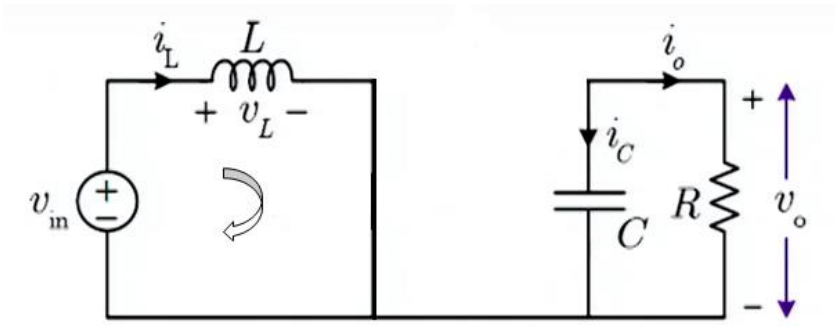

Fig.11: Switch-ON condition

By applying KVL in the left loop of Fig-11 we get,

$$L\frac{di_L}{dt} = v_{in} \tag{3.1}$$

Whereas, from the right loop of same Fig we get,

$$i_C = C\frac{dv_C}{dt} = -i_o = -\frac{v_o}{R} \tag{3.2}$$

By small ripple approximation we can write the above two equations as [32]:

$$v_L = L\frac{di_L}{dt} = < v_{in} >_{T_s} \tag{3.3}$$

$$and \ \ i_C = C\frac{dv_C}{dt} = -\frac{<v_o>_{T_s}}{R} \tag{3.4}$$

This < > signifies the average value of the voltage or current present inside it.

In this case the input current $i_{in} = i_L$ (3.5)

2. With $\bar{S}$-ON and S-OFF:

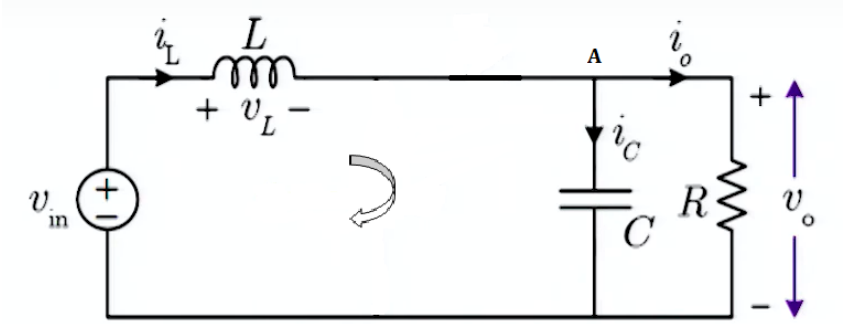

Fig.12: Switch-OFF condition

By KVL in the loop shown above we get:

$$L\frac{di_L}{dt} = v_{in} - v_o \tag{3.6}$$

By KCL at node A we get:

$$i_C = i_L - i_o = i_L - \frac{v_o}{R} \tag{3.7}$$

By small ripple approximation we can write the above two equations as [32]:

$$v_L = L\frac{di_L}{dt} = < v_{in} >_{T_s} - < v_o >_{T_s} \tag{3.8}$$

$$and \quad i_C = C\frac{dv_C}{dt} = < i_L >_{T_s} - \frac{<v_o>_{T_s}}{R} \tag{3.9}$$

In this case also the input current $i_{in} = i_L$ (3.10)

Now, by averaging the inductor voltage, capacitor current and input current from the above two cases conditions we get [32]:

- Inductor voltage: $< v_L >_{T_s} = < v_{in} >_{T_s} - (1-d) < v_o >_{T_s}$ (3.11)

  'd' signifies the average duty cycle, (1-d) is multiplied with $< v_o >_{T_s}$ because it exists only when S-OFF

- Capacitor current: $< i_C >_{T_s} = (1-d) < i_L >_{T_s} - \frac{<v_o>_{T_s}}{R}$ (3.12)

  (1-d) is multiplied with $< i_L >_{T_s}$ because it exists only when S-OFF

- Input current: $< i_{in} >_{T_s} = < i_L >_{T_s}$ (3.13)

Considering some superimposed small AC variations over DC quiescent values:

$$< v_{in} >= V_{in} + \hat{v}_{in}; < i_L >= I_L + \hat{\imath}_L; d = D + \hat{d}; < v_0 >= V_0 + \hat{v}_0; < i_{in} >= I_{in} + \hat{\imath}_{in}$$

Next, the non-linear models needs to be linearized [32].

- Perturbation of Inductor voltage equation:

$$< v_L >_{T_s} = L\frac{d< i_L >_{T_s}}{dt} =< v_{in} >_{T_s} - (1-d) < v_o >_{T_s} \quad (3.14)$$

$$=> L\frac{d(I_L + \hat{\imath_L})}{dt} = (V_{in} + \hat{v_{in}}) - \big(1 - (D + \hat{d})\big)(V_o + \hat{v_o}) \quad (3.15)$$

By solving we get:

$$L\frac{d\hat{\imath_L}}{dt} = (V_{in} + \hat{v_{in}}) + \hat{d}V_o - (1-D)[\,V_o + \hat{v_o}] \quad (3.16)$$

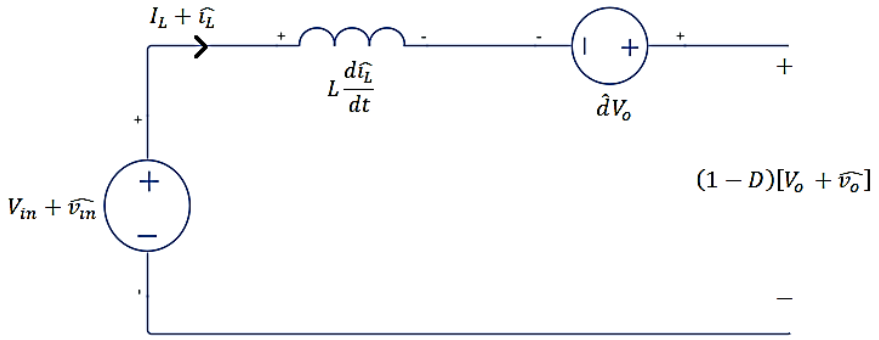

Fig.13: Inductor loop equation model

- Perturbation of Capacitor current equation:

$$< i_C >_{T_s} = C\frac{d< v_o >_{T_s}}{dt} = (1-d) < i_L >_{T_s} - \frac{< v_o >_{T_s}}{R} \quad (3.17)$$

$$=> C\frac{d(V_o + \hat{v_o})}{dt} = \big(1 - (D + \hat{d})\big)[I_L + \hat{\imath_L}] - \frac{V_o + \hat{v_o}}{R} \quad (3.18)$$

By solving we get:

$$C\frac{d\hat{v_o}}{dt} = (1-D)[I_L + \hat{\imath_L}] - \hat{d}I_L - \frac{V_o + \hat{v_o}}{R} \quad (3.19)$$

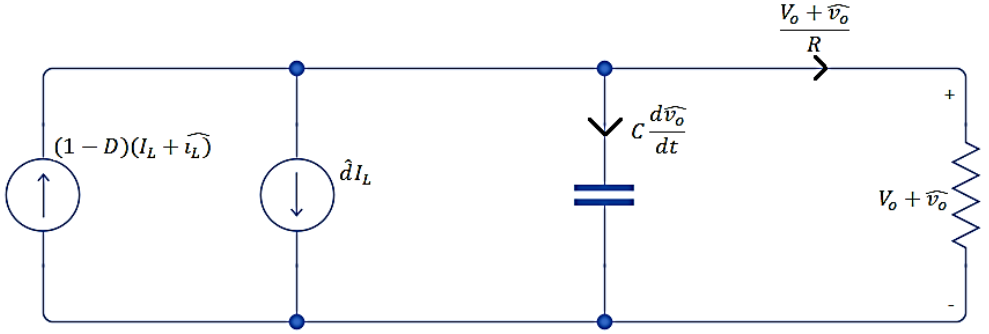

Fig.14: Capacitor node equation model

- Input current equation:

$$< i_{in} > =< i_L >_{T_s} \tag{3.20}$$

$$=> \quad I_{in} + \widehat{i_{in}} = I_L + \widehat{i_L} \tag{3.21}$$

Figures-13 and 14 and the input current equation can be now combined to form a circuit as:

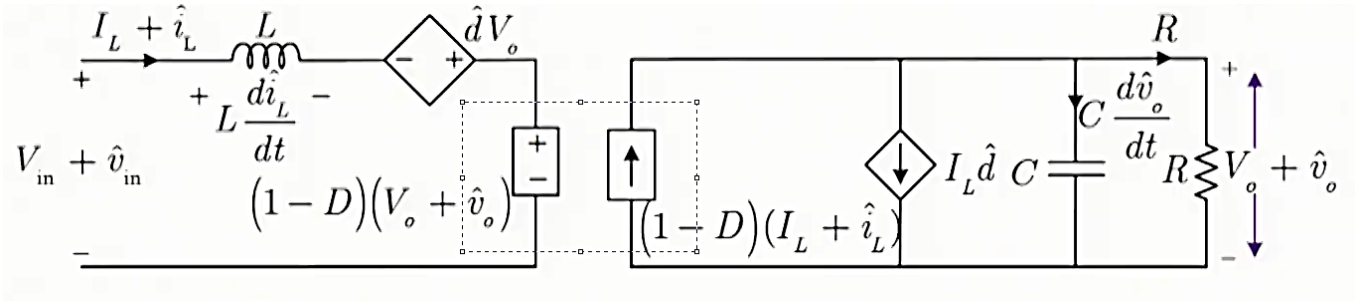

Fig.15: Small signal equivalent circuit model of boost converter (without DC transformer)

Where, the circuits can be joined by replacing the dotted portion with DC-Transformer [32]

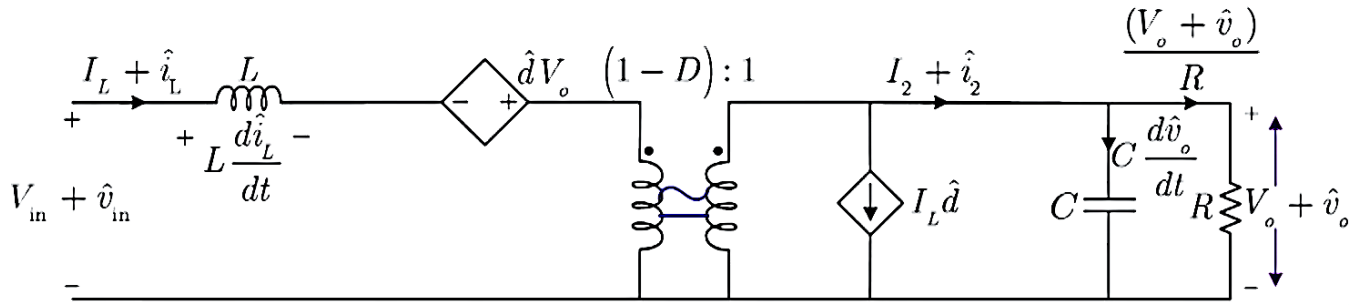

Fig.16: Small signal equivalent circuit model of boost converter

Thus the AC equivalent model will be as shown in Fig. 17:

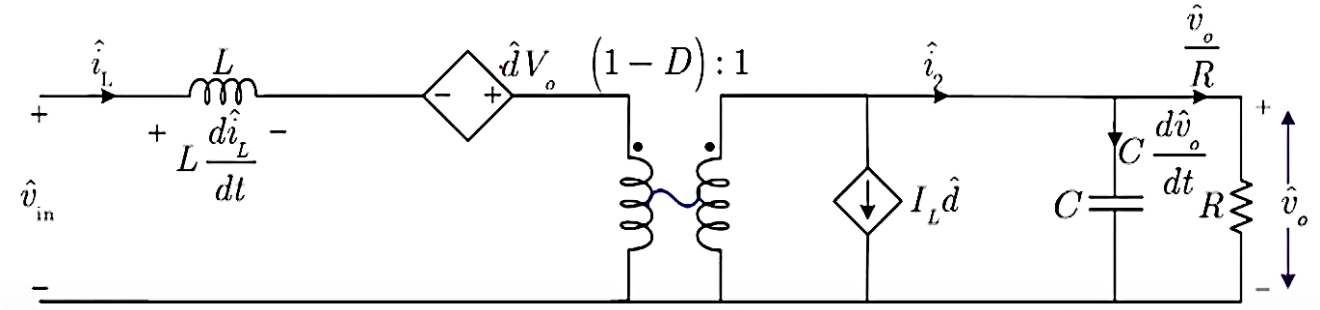

Fig.17: Small signal AC equivalent circuit model of boost converter

3.3 PI Compensation of Boost Converter:

Single PID control is often insufficient to ensure the dynamic response of both voltage and current outputs simultaneously in systems like DC-DC boost converters. Hence, a double-loop PI controller simplifies the design process as boost converters have a Right Half Plane Zero (RHPZ) structure, making their control complex. So, double-loop control addresses this issue by providing simultaneous control of both voltage and current outputs, especially double-loop PI control helps to maintain stability, especially in the face of disturbances and model uncertainties [34].

Below given are some steps on how to implement double-loop PI compensation on boost converter.

3.3.1 Finding the transfer function:

From the given Fig.17 it is clear that $\hat{V}_{in}$ and $\hat{d}$ are two major control inputs of the boost converter.

The output voltage ($\hat{V}_o$) can be expressed as the superposition of two control inputs as given below [31]:

$$\hat{V}_o(s) = G_{\hat{V}_{in}} * \hat{V}_{in}(s) + G_{\hat{d}} * \hat{d} \tag{3.22}$$

Now, $G_{\hat{V}_{in}}$ is obtained by keeping one of the control input ($\hat{V}_{in}$) active and at the same time another control input ($\hat{d}$) is deactivated.

Hence, the equivalent circuit after referring primary to secondary side we get:

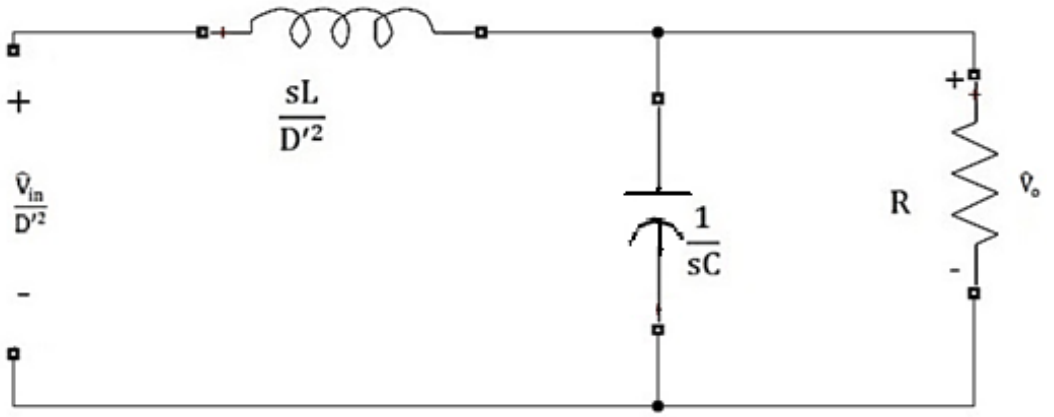

Fig.18: Equivalent circuit to find $G_{\hat{V}_{in}}$ after referring primary to secondary side

Voltage Division Rule is applied;

$$\frac{\frac{\hat{V}_o}{\hat{V}_{in}}}{D'} = \frac{R||\frac{1}{sC}}{sLD'^2+(R||\frac{1}{sC})} \tag{3.23}$$

Upon simplification, we can say;

$$G_{\hat{V}_{in}} = \frac{\hat{V}_o}{\hat{V}_{in}}\Big|\,(\hat{d}=0) = \frac{RD'}{s^2(LCR)+sL+RD'^2} \tag{3.24}$$

Now, $G_{\hat{d}}$ is obtained by keeping one of the control input ($\hat{d}$) active and at the same time deactivating another control input ($\hat{V}_{in}$)

Hence, the equivalent circuit after referring primary to secondary side we get;

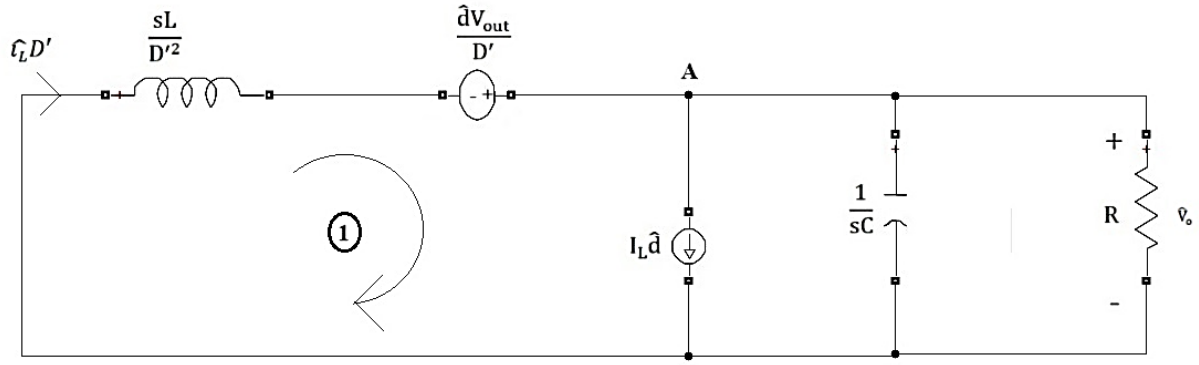

Fig.19: Equivalent circuit to find $G_{\hat{d}}$ after referring primary to secondary side

Applying nodal analysis at A;

$$\frac{\hat{V}_o}{R||\frac{1}{sC}} + I_L\hat{d} + \frac{\hat{V}_o - \frac{\hat{d}V_o}{D'}}{\frac{sL}{D'^2}} = 0 \tag{3.25}$$

Upon simplification we get [34];

$$G_{\hat{d}} = \frac{\hat{V}_o}{\hat{d}}\Big|(\hat{V}_{in}=0) = \frac{RD'V_o - sRLI_L}{s^2(LCR)+sL+RD'^2} \tag{3.26}$$

Now, during the double loop DC-DC boost converter design, the output voltage ($\hat{V}_o$) and the inductor current ($\hat{i}_L$) have to be measured. Therefore, the open-loop transfer functions "G_1" and "G_2" are derived respectively in the following equations.

Transfer function "G_1" between inductor current and duty ratio $\frac{\hat{i}_L}{\hat{d}}\Big|(\hat{V}_{in}=0)$ is also obtained from Fig-19 by keeping control input ($\hat{d}$) active and at the same time deactivating another control input ($\hat{V}_{in}$).

Applying KCL at point A;

$$-\hat{i}_L D' + I_L \hat{d} + \frac{\hat{V}_o}{R||\frac{1}{sC}} = 0 \tag{3.27}$$

Upon simplification we get;

$$\hat{V}_o = \frac{\hat{i}_L R - I_L \hat{d} R}{sRC+1} \tag{3.28}$$

Applying KVL at loop 1;

$$\frac{\hat{d} V_o}{D'} - \frac{\hat{i}_L sL}{D'^2} - \hat{V}_o = 0 \tag{3.29}$$

Upon simplification and by replacing $\hat{V}_o$ from eqn. (3.29) we get [34];

$$G_1 = \frac{\hat{i}_L}{\hat{d}} \Big| (\hat{V}_{in} = 0) = \frac{sV_o C + 2I_L D'}{s^2 LC + \frac{sL}{R} + D'^2} \tag{3.30}$$

Similarly, transfer function between output voltage and the inductor current "G_2" is obtained from Fig-20 [34]:

$$G_2 = \frac{G_{\hat{d}}}{G_1} = \frac{\frac{\hat{V}_o}{\hat{d}}}{\frac{\hat{i}_L}{\hat{d}}} = \frac{\hat{V}_o}{\hat{i}_L} | (\hat{V}_{in} = 0) = \frac{D' V_o - sLI_L}{sV_o C + 2D' I_L} \tag{3.31}$$

Substituting values of all defined terms in transfer functions "G_1" and "G_2" they can be expressed as

$$G_1 = \frac{\hat{i}_L}{\hat{d}} \Big| (\hat{V}_{in} = 0) = \frac{0.0023544s + 0.3034}{s^2(6.4*10^{-8}) + s(0.00004) + 0.25} \tag{3.32}$$

$$G_2 = \frac{\hat{V}_o}{\hat{i}_L} | (\hat{V}_{in} = 0) = \frac{14.715 - 0.0024272s}{0.00023544s + 0.3034} \tag{3.33}$$

By observing the transfer function "G_2" it can be said that the outer-loop of boost converter has a Right Half Plane Zero (RHPZ) structure, hence double-loop PI control is applied to ease the complexity that occurs due to presence of a Right Half Plane Zero.

3.3.2 Double-loop Control:

Double-loop control is implemented using PI controllers for both the current (inner-loop) as well as the voltage (outer-loop). The PI parameters are calculated to ensure that the system response meets desired transient characteristics. Firstly, inner current loop is compensated with

the help of PI controller "C_1" and then the outer-loop is compensated with the help of PI controller "C_2" which is attached to outer-loop [33].

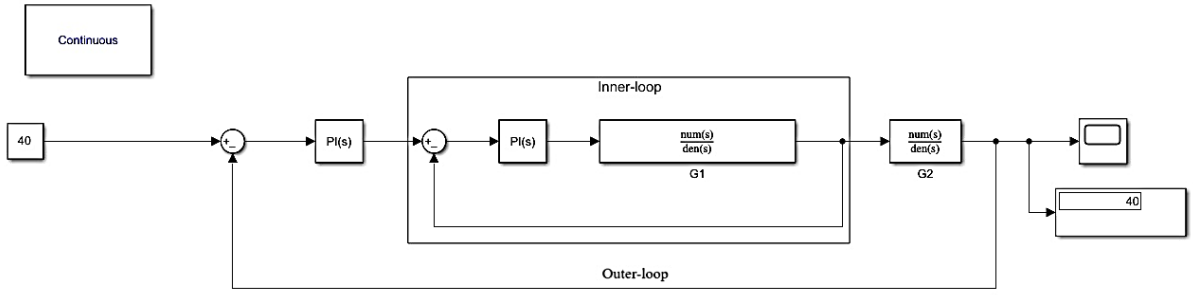

Fig-20: Double-loop PI structure of a boost converter in continuous time

Inner-loop transfer function "G_1" is compensated by using PI controller "C_1" such that,

$$C_1 = K_{P_1} + \frac{K_{I_1}}{s} = 0.10339 + \frac{1.0339}{s} \tag{3.34}$$

Next, the outer-loop is compensated by using the PI controller "C_2"

$$C_2 = K_{P_2} + \frac{K_{I_2}}{S} = 0.01561 + \frac{0.09395}{s} \tag{3.35}$$

Compensating both the inner-loop and outer-loop with the help of PI controllers "C_1" and "C_2" respectively, we are able to obtain a stable output which follows the reference accurately, as shown in Fig. 21, which can be observed through both the scope output and the display output.

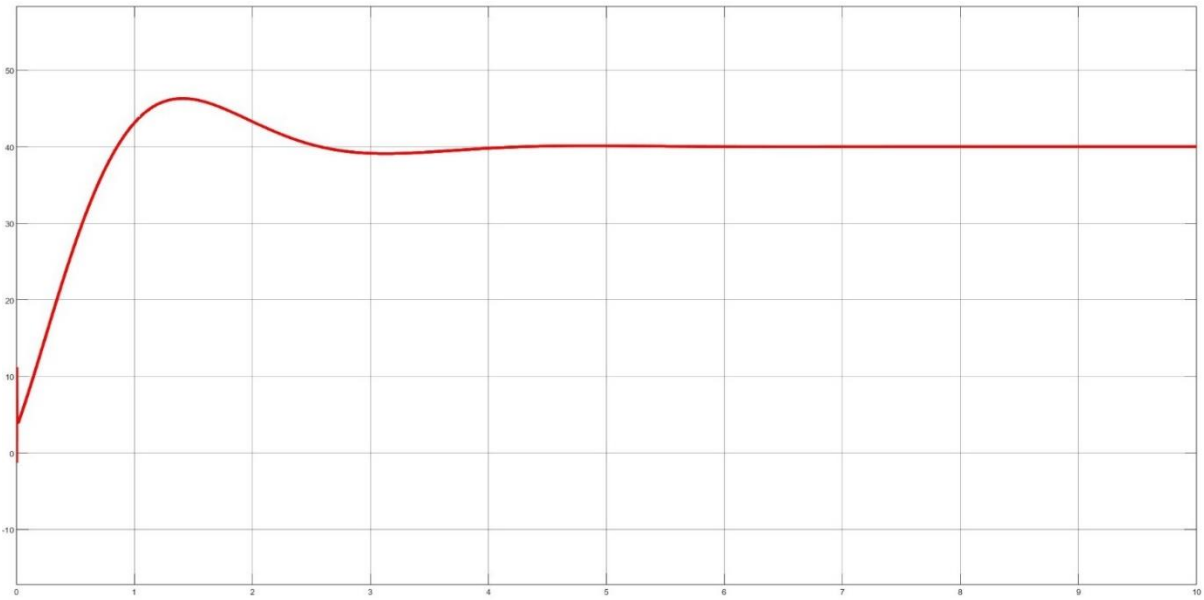

Fig-21: Response of double-loop PI compensation of boost converter in continuous time

In order to, discretize the entire system a sample time of $T_s = 2.5\times10^{-6}$ seconds is chosen. The choice is made to incorporate 10 samples per 40kHz switching frequency of the converter.

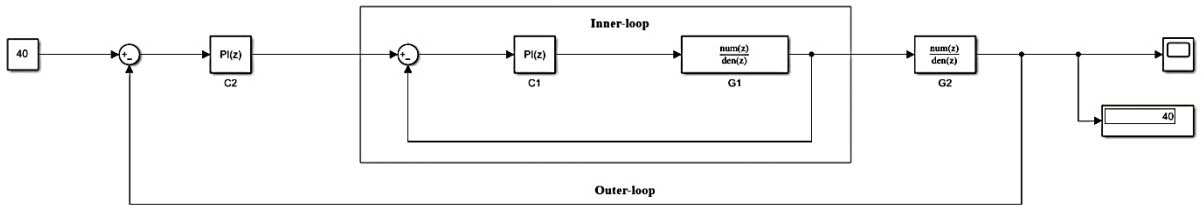

Fig.22: Double-loop PI structure of a boost converter in discrete time

After discretization, Inner-loop transfer function can be written as,

$$G_1(z) = \frac{0.091911z - 0.091911}{z^2 - 1.998z + 0.9984} \tag{3.36}$$

Similarly, outer-loop transfer function can be written as,

$$G_2(z) = \frac{-10.279z + 10.433}{z - 0.9968} \tag{3.37}$$

Inner-loop transfer function "G_1" is compensated by using PI controller "C_1" such that,

$$C_1 = K_{P_1} + K_{I_1}\frac{T}{z-1} = 24.962 + \frac{14.3332}{z-1} \tag{3.38}$$

Consequently, the outer-loop is compensated by using the PI controller "C_2"

$$C_2(z) = K_{P_2} + K_{I_2}\frac{T}{z-1} = 3.5884 * 10^{-5} + \frac{1.07652*10^{-5}}{z-1} \tag{3.39}$$

Thus, the output response can be seen by the help of a scope which shows successful PI compensation after discretization of the plant.

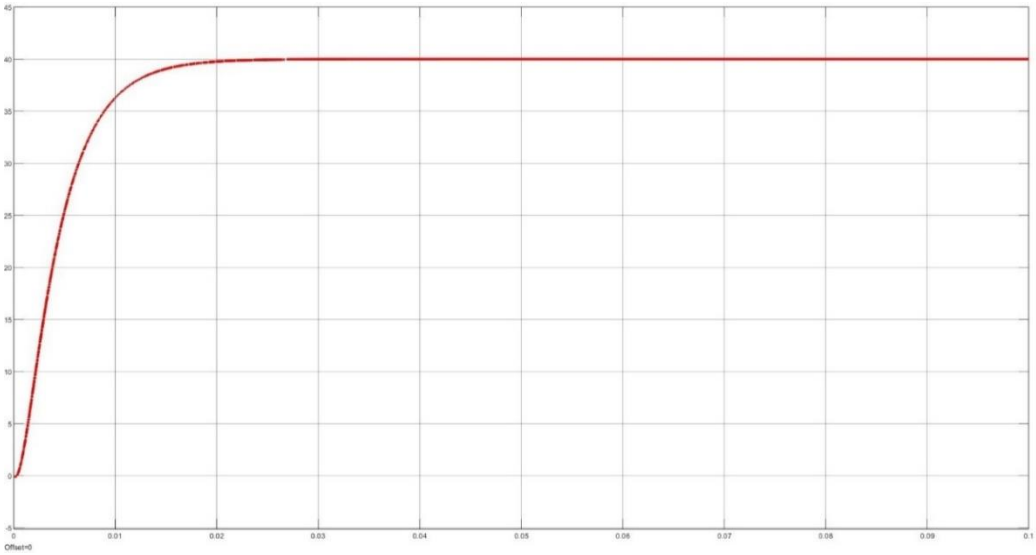

Fig.23(a): Response of double-loop PI compensation of boost converter in discrete time

The root locus of the double-loop PI-compensation of the boost converter is:

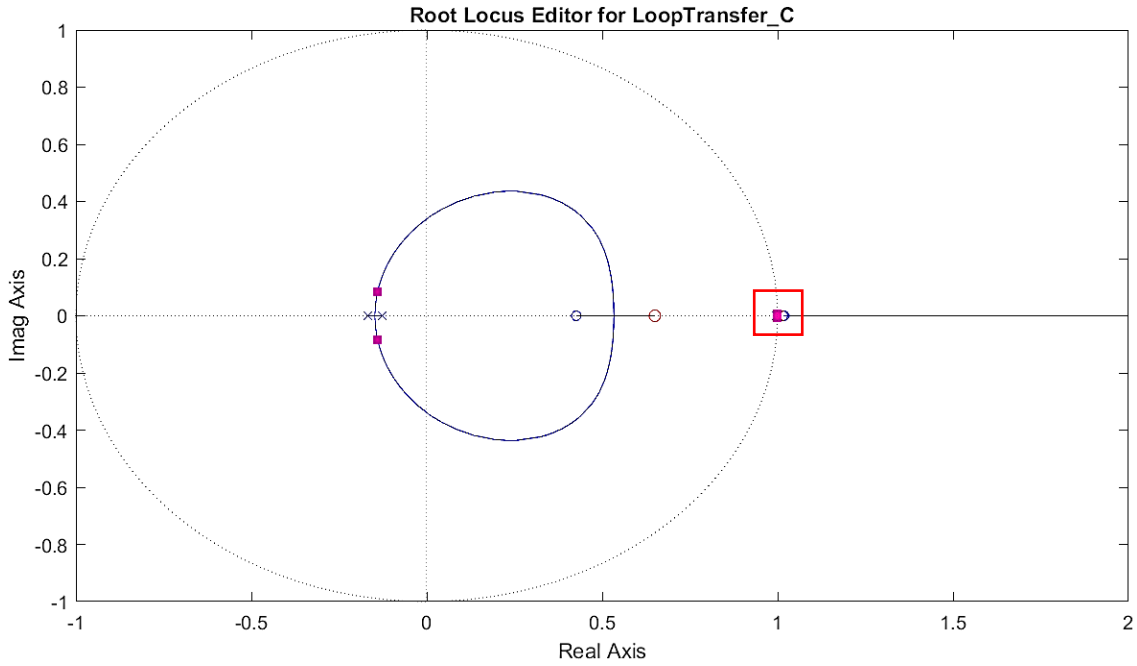

Fig. 23(b): Root Locus for PI compensated outer loop

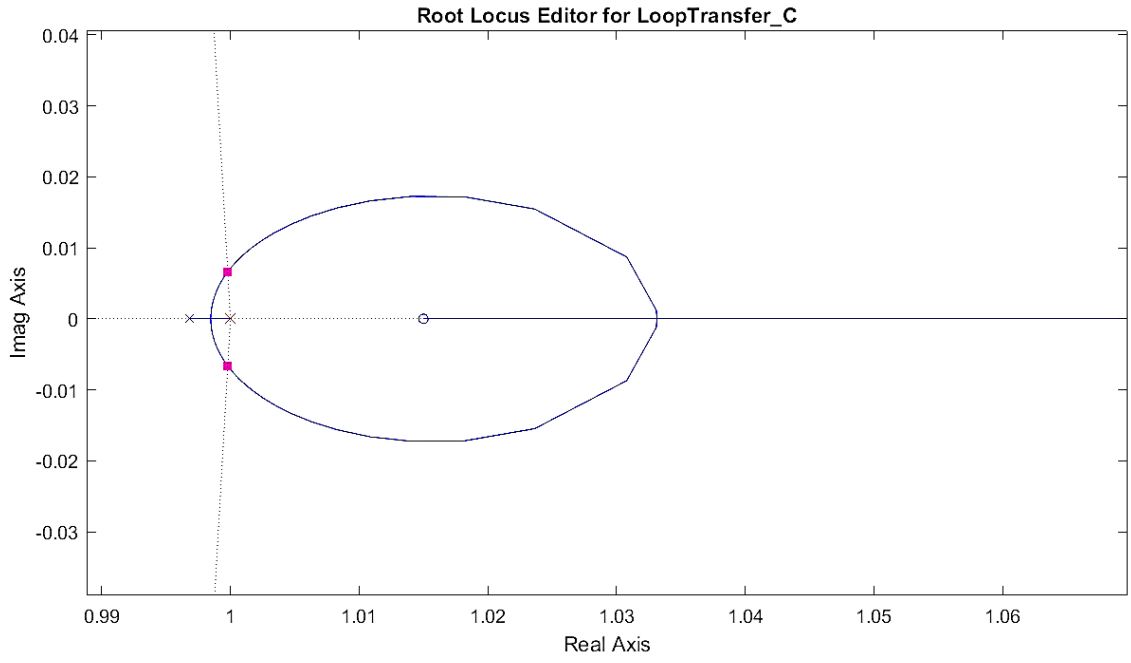

Fig. 23(c): Zoomed-in portion of the Root Locus of Fig. 23(b)

As can be obtained from the root locus the GM i.e. the maximum gain for stability for the double-loop PI-compensated system will be 0.00080629.

Now, the double loop PI controller is implemented in Simscape model of the Boost converter by taking current and voltage measurement for inner-loop and outer-loop, respectively and keeping all the values of different components intact [34].

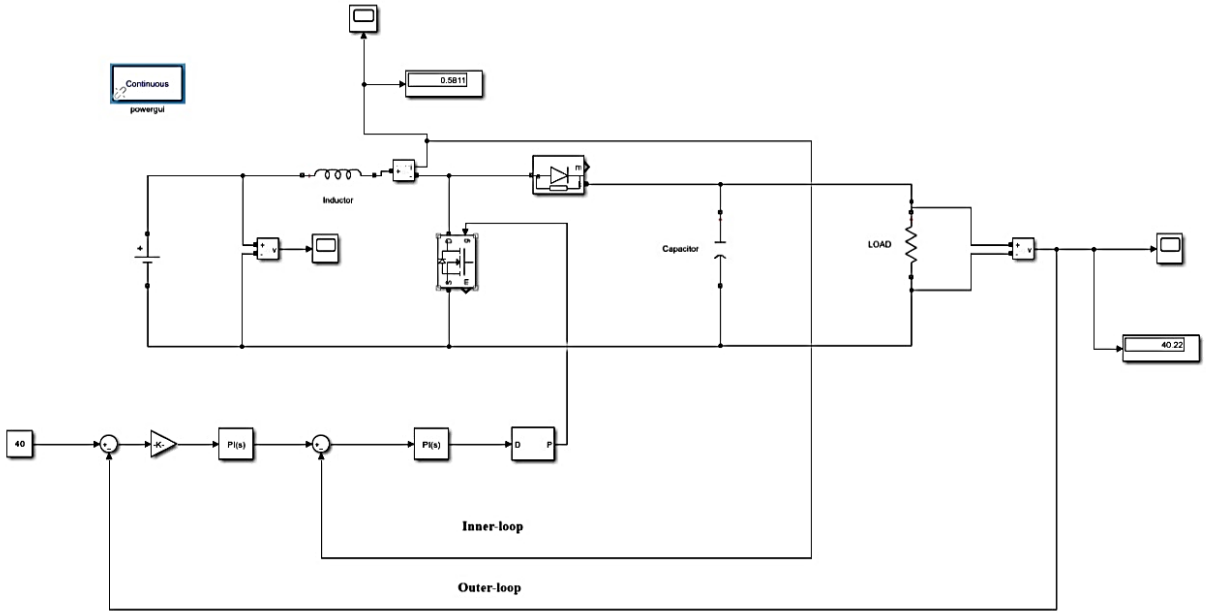

Fig.24: Simscape model of double-loop PI compensation of boost converter

Keeping the PI controller gain same as we kept for continuous transfer function in both inner-loop as well as outer-loop, such as

$$C_1 = K_{P_1} + \frac{K_{I_1}}{s} = 0.10339 + \frac{1.0339}{s} \tag{3.40}$$

$$C_2 = K_{P_2} + \frac{K_{I_2}}{s} = 0.01561 + \frac{0.09395}{s} \tag{3.41}$$

The output response tries to follow the reference value as shown in Fig. 25.

Fig.25: Response of Simscape model of double-loop pi compensation of boost converter

Hence, we can say from these responses it is evident that after double-loop PI compensation of boost converter the output tries to follow the reference given.

3.3.3 Limitations of Boost Converters

The presence of a right-half-plane (RHP) zero is a significant limitation in boost converters, especially in control design and system performance. Here's an overview of the key limitations imposed by the RHP zero:

1. Reduced Control Bandwidth leading to **Slower Response** and **Delayed Settling Time**

2. Stability Challenges: Complex Control Design and a reduction in **Phase Margin**

3. Limited Load Regulation against **Dynamic Load Changes**: Due to the RHP zeros when the load changes rapidly, the boost converter may struggle to adjust the output voltage quickly, leading to temporary deviations from the desired voltage level.

4. Design Trade-offs as in the form of **Gain and Bandwidth Trade-off**

5. Energy Efficiency Implications: The phase lag and slower response time can lead to less efficient energy transfer during transient conditions, as the converter cannot react as quickly to changes in input or load conditions.

6. Impact on Maximum Power Point Tracking (MPPT) Performance: In applications like wind or solar energy, where MPPT is crucial, the RHP zero can hinder the ability to quickly track the maximum power point, reducing the overall energy capture efficiency. The slow response necessitated by the RHP zero means the system may not adapt quickly enough to changes in environmental conditions.

One of the most popular means of mitigating the ill-effects of the RHP zeros is to employ periodic or multi-rate control to relocate the loop zeros at suitable locations leading to improved robustness.

Chapter 4

Multi/2-Rate Control from a 2-Periodic Perspective: A Review

4.1 Limitation of LTI controllers

The Linear Time-Invariant (LTI) controller is widely recognized and commonly used in both research and industrial applications because it is relatively simple to analyse and design without introducing significant complexity. Many methods have been developed in control system engineering specifically for designing LTI controllers [17], [18], [20], [21], and they continue to be a preferred option in various industrial settings due to their straightforward nature. However, despite these advantages, LTI controllers do have some limitations, such as:

1. Open loop zeros cannot be placed arbitrarily
2. Robust compensation cannot be achievable for the plant with NMP poles and zeros
3. Arbitrary high GM cannot be achieved, due to the presence of NMP zeros

Thus an LTI controller cannot overcome the difficulties caused by non-minimum phase(NMP) zeros. For plants with unstable poles and NMP zeros an LTI controller cannot ensure adequate robustness. Moreover, if the NMP zero and the unstable pole are at close vicinity then the robustness becomes even worse. Moreover, pole-zero cancellation cannot be used for safeguarding the internal stability. In this regard, periodic controller and multi-rate control can be beneficial, as they can be designed in such a way that zero placement can be achieved, thus improving the robustness by relocating the NMP loop-zeros at any arbitrary locations.

The periodic time-varying controllers have advantages over time-invariant controllers to stabilize the plant as well as to improve its robustness. The periodic control or a generalized multi-rate control i.e. multi-rate control from a 2-periodic perspective can place loop zeros arbitrarily and consequently the improved GM can be achieved compared to LTI controllers [17], [19], [20].

4.2 2-Periodic controller

For an n-th order, SISO, LDTI plant $G(z) = k\frac{b(z)}{a(z)}$, r < n, with

$$a(z) = z^n + a_{n-1}z^{n-1} + \cdots + a_1 z + a_0 \tag{4.1}$$

$$b(z) = b_r z^r + b_{r-1}z^{r-1} + \cdots + b_1 z + b_0 \tag{4.2}$$

Consider, following [17], the 2-periodic, m-th order controller shown in Fig.26 , where D_i and C_i are 2-periodically time varying gains, which can be described in the form of discrete Fourier series as,

$$D_i(N) = d_{i,0} + (-1)^N d_{i,1}, \quad i = 0,1,\ldots m \tag{4.3}$$

$$C_i(N) = c_{i,0} + (-1)^N c_{i,1}, \quad i = 0,1,\ldots (m-1) \tag{4.4}$$

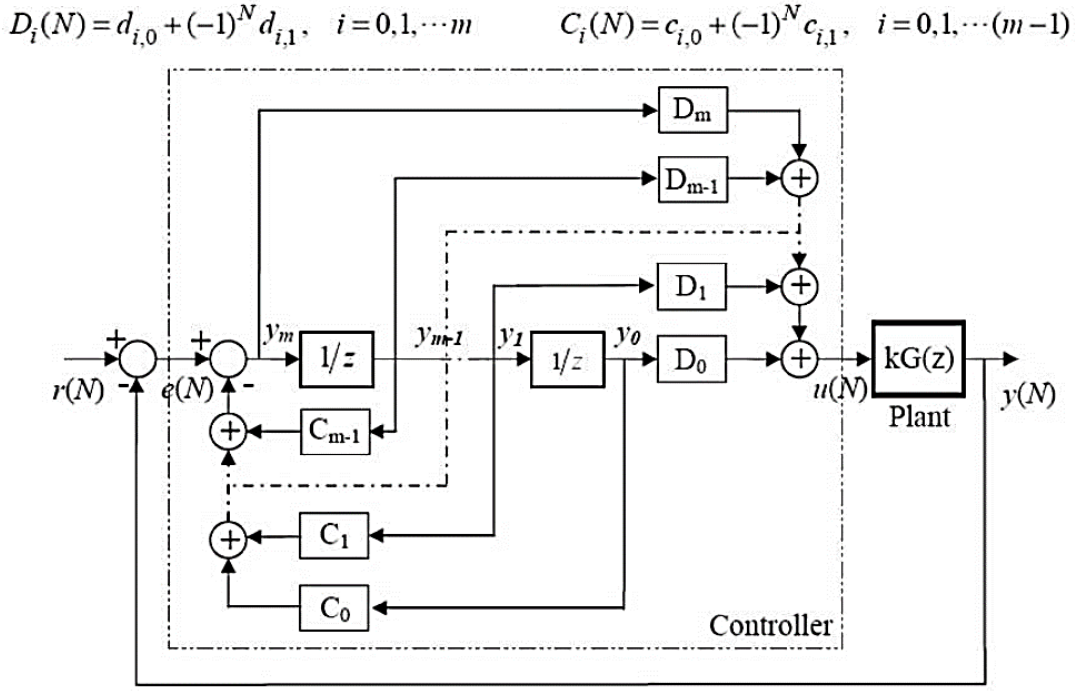

Fig.26 :The 2-Periodic controller in 1-DOF form and the LTI plant

The equivalent periodic coefficient transfer function corresponding to the controller is,

$$C(z,N) \triangleq [Q(z,N)][P(z,N)]^{-1}$$
$$= [D_m z^m + D_{m-1} z^{m-1} + \cdots + D_0][z^m + C_{m-1} z^{m-1} + \cdots C_0]^{-1} \quad (4.5)$$

With

$$Q(z,N) \triangleq Q_0(z) + (-1)^N Q_1(z)$$
$$= \left[d_{m,0} z^m + \cdots + d_{0,0}\right] + (-1)^N [d_{m,1} z^m + \cdots + d_{0,1}] \quad (4.6)$$

$$P(z,N) \triangleq P_0(z) + (-1)^N P_1(z)$$
$$= \left[z^m + c_{m-1,0} z^{m-1} + \cdots + c_{0,0}\right] + (-1)^N [c_{m-1,1} z^{m-1} + \cdots + c_{0,1}] \quad (4.7)$$

Several methods are reported in the literature that can be employed to analyse a 2-periodic system. Such as, Floquet Theory, Frequency-lifted Reformulation, Cyclic Reformulation and Time-lifted Reformulation. In this work we will use the Time-lifted reformulation technique.

4.2.1 Time-lifting method

Time-domain lifting technique has the advantage of representing a SISO M-periodic system to an equivalent M-input M-output LDTI system, producing a M×M transfer matrix. It is to be noted that any LDTI system can be considered to be a 2-Periodic one and consequently it can be transformed into a MIMO time-invariant form. In 2-periodic system, coefficients of all the even and odd instants are similar. So, a SISO, causal, 2-periodic map g can be lifted to a 2-input 2-output time invariant representation. As a result, it makes the lifted system expressed as even and odd instant LDTI systems. Let us consider e(0), e(1), e(2),..... be the sequence of inputs and u(0), u(1), u(2),….. be the corresponding output sequences [22]. Now, lifting the system to even and odd instants inputs and outputs and representing them in the transform domain as,

$$E_e(z^2) = \sum_{i=0}^{\infty} z^{-2i} e(2i) \tag{4.8}$$

$$z^{-1}E_o(z^2) = \sum_{i=0}^{\infty} z^{-2i-1} e(2i+1) \tag{4.9}$$

$$U_e(z^2) = \sum_{i=0}^{\infty} z^{-2i} u(2i) \tag{4.10}$$

$$z^{-1}U_o(z^2) = \sum_{i=0}^{\infty} z^{-2i-1} u(2i+1) \tag{4.11}$$

The even and odd instant input and output sequences can be written as,

$$E(z) = E_e(z^2) + z^{-1}E_o(z^2) \tag{4.12}$$

$$U(z) = U_e(z^2) + z^{-1}U_o(z^2) \tag{4.13}$$

where,

$E(z)$ = The z-transform of complete input sequence,

$E_e(z^2)$ = The z-transform of even instant of the input sequence

$z^{-1}E_0(z^2)$= The z-transform of even instant of the input sequence,

$U(z)$ = The z-transform of complete output sequence,

$U_e\,(z^2)$ = The z-transform of even instant of the output sequence,

$z^{-1}U_0(z^2)$ = The z-transform of even instant of the output sequence.

Now, the even and odd instant outputs can be linked to the even and odd instant inputs as,

$$\begin{bmatrix} U_e(z^2) \\ z^{-1}U_o(z^2) \end{bmatrix} = \tilde{G}(z^2) \begin{bmatrix} E_e(z^2) \\ z^{-1}E_o(z^2) \end{bmatrix} \tag{4.14}$$

with,

$$\tilde{G}(z^2) = \begin{bmatrix} G_{11}(z^2) & z^{-1}G_{12}(z^2) \\ z^{-1}G_{21}(z^2) & G_{22}(z^2) \end{bmatrix} \tag{4.15}$$

Where each G_{ij} (for i, j = 1,2) is a LDTI, proper transfer function in z^2.

$\tilde{G}(z^2)$ is the lifted LDTI transfer matrix that satisfies the causality condition that $\tilde{G}(\infty)$ is lower triangular, which is the necessary and sufficient condition for the transfer function to be realizable as SISO 2-periodic system.

4.2.2 Closed Loop Characteristic Equation

Let, for any polynomial $f(z)$, $f^{+}=f(z)$ and $f^{-}=f(-z)$.

Time domain lifting theory is applied to the controller and the plant. The transfer matrix of the polynomial $Q(z)$ becomes [17],[22]

$$\bar{Q}(z^2) = \begin{bmatrix} Q_{11}(z^2) & z^{-1}Q_{12}(z^2) \\ zQ_{21}(z^2) & Q_{22}(z^2) \end{bmatrix} \tag{4.16}$$

Where,

$$\left.\begin{aligned} Q_{11} &= Q_0^+ + Q_0^- + Q_1^+ + Q_1^- \\ Q_{12} &= Q_0^+ - Q_0^- + Q_1^+ - Q_1^- \\ Q_{21} &= Q_0^+ - Q_0^- - Q_1^+ + Q_1^- \\ Q_{22} &= Q_0^+ + Q_0^- - Q_1^+ - Q_1^- \end{aligned}\right\} \tag{4.17}$$

The lifted transfer matrix of the polynomial $P(z)$,

$$\bar{P}(z^2) = \frac{1}{2}\begin{bmatrix} P_{11}(z^2) & z^{-1}P_{12}(z^2) \\ zP_{21}(z^2) & P_{22}(z^2) \end{bmatrix} \tag{4.18}$$

where,

$$\left.\begin{aligned} P_{11} &= P_0^+ + P_0^- + P_1^+ + P_1^- \\ P_{12} &= P_0^+ - P_0^- + P_1^+ - P_1^- \\ P_{21} &= P_0^+ - P_0^- - P_1^+ + P_1^- \\ P_{22} &= P_0^+ + P_0^- - P_1^+ - P_1^- \end{aligned}\right\} \quad (4.19)$$

As we know, controller transfer function is $C(z,N)= [Q(z)][P(z)]^{-1}$

So, from (4.16) and (4.18),

$$\bar{C}(z^2) = \frac{1}{\Delta_c}\begin{bmatrix} C_{11}(z^2) & z^{-1}C_{12}(z^2) \\ zC_{21}(z^2) & C_{22}(z^2) \end{bmatrix} \quad (4.20)$$

Where,

$$\left.\begin{aligned} \Delta_c &= 4(P_0^+P_0^- - P_1^+P_1^-) \\ C_{11} &= Q_0^+P_0^- + Q_0^-P_0^+ - Q_0^+P_1^- - Q_0^-P_1^+ + Q_1^+P_0^- + Q_1^-P_0^+ - Q_1^+P_1^- - Q_1^-P_1^+ \\ C_{12} &= Q_0^+P_0^- - Q_0^-P_0^+ + Q_0^+P_1^- - Q_0^-P_1^+ + Q_1^+P_0^- - Q_1^-P_0^+ + Q_1^+P_1^- - Q_1^-P_1^+ \\ C_{21} &= Q_0^+P_0^- - Q_0^-P_0^+ - Q_0^+P_1^- + Q_0^-P_1^+ - Q_1^+P_0^- + Q_1^-P_0^+ + Q_1^+P_1^- - Q_1^-P_1^+ \\ C_{22} &= Q_0^+P_0^- + Q_0^-P_0^+ + Q_0^+P_1^- + Q_0^-P_1^+ - Q_1^+P_0^- - Q_1^-P_0^+ - Q_1^+P_1^- - Q_1^-P_1^+ \end{aligned}\right\} \quad (4.21)$$

Now, the lifted transfer matrix of the plant is

$$\tilde{G}(z^2) = \begin{bmatrix} G_{11}(z^2) & z^{-1}G_{12}(z^2) \\ z^{-1}G_{21}(z^2) & G_{22}(z^2) \end{bmatrix} \quad (4.22)$$

Where,

$$\left.\begin{aligned} G_{11} &= G_{22} = b^+a^- + b^-a^+ \\ G_{12} &= G_{21} = b^+a^- - b^-a^+ \end{aligned}\right\} \quad (4.23)$$

The characteristic equation of the overall system (i.e. including the 2-periodic controller and the plant) is given by

$$\Delta = det[I+K\tilde{G}\bar{C}] \quad (4.24)$$

Substituting the values of 2×2 transfer matrices of $\tilde{G}$ and $\bar{C}$ from equation (4.20) and (4.22) to the characteristic equation of (4.24), we get,

$$\begin{aligned} \Delta = {} & a^+a^-(P_0^+P_0^- - P_1^+P_1^-) + K\,[b^+a^-(Q_0^+P_0^- - Q_1^-P_1^+) + b^-a^+(Q_0^-P_0^+ - Q_1^+P_1^-)] \\ & + K^2b^+b^-(Q_0^+Q_0^- - Q_1^+Q_1^-) = 0 \end{aligned} \quad (4.25)$$

4.2.3 Loop Zero Placement

From the characteristic equation of (4.25), the plant zeros are the co-efficient of K^2 term. Due to the presence of term, loop-zeros cannot be placed arbitrarily. But coefficient of K term does not contain such term and roots of this coefficient can be assigned to the required places.

Therefore, if coefficient of K^2 term is made equal to zero then coefficient of K term would determine the locations of loop-zeros. Consequently, achieving the loop-zero placement. To make the K^2 term equal to zero, the following four conditions are used [40],

i. $Q_0^+ = Q_1^-$
ii. $Q_0^+ = -Q_1^-$
iii. $Q_0^+ = Q_1^+$
iv. $Q_0^+ = -Q_1^+$

The equation (4.25) now becomes,

$$\Delta = a^+a^-(P_0^+P_0^- - P_1^+P_1^-) + K\,[b^+a^-(Q_0^+P_0^- - Q_1^-P_1^+) + b^-a^+(Q_0^-P_0^+ - Q_1^+P_1^-) \quad (4.26)$$

The above equation can be written as,

$$\hat{A}(z^2)\hat{P}(z^2) + k\tilde{Z}(z^2) = \hat{\Delta}(z^2) = \breve{\Delta}(z^2)\breve{D}(z^2) = 0 \quad (4.27)$$

Where,

$\hat{A}(z^2)$ = Plant poles = a^+a^-
$= a_0 + a_2z^2 + \cdots + (-1)^n z^{2n}$ (4.28)

$\hat{P}(z^2)$ = Controller poles = $(P_0^+P_0^- - P_1^+P_1^-)$
$= \hat{p}_0 + \hat{p}_2z^2 + \cdots + (-1)^m z^{2m}$ (4.29)

$\hat{Z}(z^2)$ = Zero polynomial of the overall system
$= K\,[b^+a^-(Q_0^+P_0^- - Q_1^-P_1^+) + b^-a^+(Q_0^-P_0^+ - Q_1^+P_1^-)]$
$= r_0 + r_2z^2 + \cdots + r_{2\theta}z^{2\theta}$ (4.30)

$\breve{\Delta}(z^2)$ = Desired closed loop poles

$\breve{D}(z^2)$ = Additional closed loop poles

From the above equations it can be noted that the controller pole polynomial and the loop-zero polynomial both are assignable. So, by adjusting the parameters of zero polynomial, zero placement can be achieved.

4.2.4 Order of Controller

It can be observed from (4.27), the degree of polynomials $\hat{A}(z^2)$ and $\hat{P}(z^2)$ are $2n$ and $2m$ respectively. The degree of the polynomial $\hat{Z}(z^2)$ can be defined as,

$$\theta = m + \eta \;\; with\, \eta = n - I^{+}\{\tfrac{n-r}{2}\} \tag{4.31}$$

where,

I^{+} is the ceiling operator,

θ is the total number of assignable loop-zeros,

η is the assignable plant zeros which depends upon the relative order of the plant.

From (4.6), (4.7) and (4.29), the total number of assignable coefficients is ($2m$+m) to place m controller poles and (m+ η) loop zeros. The order of the controller is defined by,

$$m \geq \eta = n - I^{+}\{\tfrac{n-r}{2}\} \tag{4.32}$$

Note that for plants of relative order either 1 or 2 one requires $m \geq n - 1$

4.2.5 Evaluation of Controller Parameters

Controller parameters are evaluated by solving the characteristic equation. The controller is synthesized using approach of [17]. It is a two-stage method. In stage-I, an intermediate polynomial is obtained and in stage-II, controller parameters are calculated from the intermediate polynomial.

Stage-I

Let,

$$\hat{B}(z) = b^{+}a^{-} = [\hat{b}_0 + \hat{b}_2 z^2 + \cdots + \hat{b}_{2\varphi_1} z^{2\varphi_1}] + z[\hat{b}_1 + \hat{b}_3 z^2 + \cdots + \hat{b}_{2\varphi_2+1} z^{2\varphi_2}] \quad (4.33)$$

$$= \hat{B}_e(z^2) + z\hat{B}_d(z^2) \quad (4.34)$$

With $\varphi_1 = I^{-}\{\frac{n+r}{2}\}$ and $\varphi_2 = I^{-}\{\frac{n+r-1}{2}\}$

$$\hat{L}(z) = (Q_0^{+}P_0^{-} - Q_1^{-}P_1^{+})$$

$$= [\hat{l}_0 + \hat{l}_2 z^2 + \cdots + \hat{l}_{2m} z^{2m}] + z[\hat{l}_1 + \hat{l}_3 z^2 + \cdots + \hat{l}_{2m-1} z^{2(m-1)}] \quad (4.35)$$

$$= \hat{L}_e(z^2) + z\hat{L}_d(z^2) \quad (4.36)$$

From (4.34), (4.36) we obtain,

$$\hat{Z}(z^2) = \hat{B}^{+}\hat{L}^{+} + \hat{B}^{-}\hat{L}^{-} = 2\hat{B}_e(z^2)\hat{L}_e(z^2) + 2z^2\hat{B}_d(z^2)\hat{L}_d(z^2) \quad (4.37)$$

$$= r_0 + r_2 z^2 + \cdots + r_{2\theta} z^{2\theta} \quad (4.38)$$

Now, using (4.34), (4.36) and (4.38) the Sylvester matrix like equation is obtained below,

$$\begin{bmatrix} r_0 \\ r_2 \\ r_4 \\ \vdots \\ r_{2\theta} \end{bmatrix} = \begin{bmatrix} \hat{b}_0 & \cdots & 0 & 0 & \cdots & 0 \\ \hat{b}_2 & \cdots & 0 & \hat{b}_1 & \cdots & 0 \\ \hat{b}_4 & \cdots & 0 & \hat{b}_3 & \cdots & 0 \\ \vdots & \ddots & \vdots & \vdots & \ddots & \vdots \\ 0 & \cdots & \hat{b}_{2\varphi_1} & 0 & \cdots & \hat{b}_{2\varphi_2+1} \end{bmatrix} \begin{bmatrix} \hat{l}_0 \\ \vdots \\ \hat{l}_{2m} \\ \hat{l}_1 \\ \vdots \\ \hat{l}_{2m-1} \end{bmatrix} \quad (4.39)$$

Now, from (4.38) we can say that (4.40) will be a consistent set of equations if the following conditions are satisfied [24]:

1. If the plant has a pole-zero cancelation at p then the effective loop transfer function would have the same at p^2, signifying that the loop-zero polynomial must have a root at p^2. (Clearly, for internal stability, the plant should not have any unstable pole-zero cancelation at p, when $|p|<1$)

2. If the plant denominator has an even factor (z^2+c), then also the loop transfer function would have a pole-zero cancelation at $-c$, and so the loop-zero polynomial must contain the same factor. (Again, for internal stability, $|c|<1$ must be satisfied.)
3. If the plant numerator has an even factor (z^2+c), then the loop-zero polynomial must also contain the same.

Equation (4.39) is solved using matrix inversion method and the $\hat{L}(z)$ polynomial is obtained. But the matrix $\bar{B}$ may become singular for the following cases:

i. If the plant has pole(s) or zero(s) at origin.

ii. If the plant has a pole-zero cancelation at origin.

iii. If the denominator and numerator contains only even factors.

All these cases will lead to some all-zero identities, which will make (4.39) an undeterminable but consistent set of linear equations.

Assume rank of $\bar{B}$= rank of $[\bar{B} \mid \bar{r}]$; then the equation (4.39) becomes consistent and the polynomial $\hat{L}(z)$ can be obtained.

Stage-II

Polynomial $\hat{L}(z)$ which is obtained in stage-I, now, will be divided into two parts for all four conditions $Q_0^+ = \pm Q_1^{\pm}$ and will be suitably assigned to pole polynomials to calculate the controller parameters.

Condition-1: $Q_0^+ = Q_1^-$

From (4.36) we get,

$$\hat{L}(z) = Q_0^-(P_0^+ - P_1^-) \tag{4.40}$$

Then, to find Q_0^- and $(P_0^+ - P_1^-)$, polynomial $\hat{L}(z)$ is divided into two parts such that

i. Both the halves are real polynomials (i.e., a complex root and its conjugate should be present in the same half).

ii. At least one of the halves has no even factor [17].

If the factor that satisfies the 2nd condition is, in addition, monic, then the same can be chosen as $(P_0^+ - P_1^-)$ and the rest would be Q_0^- . Values of $d_{i,0}$ and $d_{i,1}$ (for i = 0, 1,…,m) can be directly

obtained from Q_0^- and Q_1^+ . Calculations for finding $c_{i,0}$ and $c_{i,1}$ (for i = 0, 1,…,m-1) are shown below.

Let,

$$(P_0^+ - P_1^-) = \Gamma(z) = \gamma_0 + \gamma_1 z + \cdots + \gamma_m z^m \qquad (4.41)$$

From (4.7) and (4.41) it is obtained,

$$P_0^+\Gamma^- + P_0^-\Gamma^+ = \hat{P}(z^2) + \Gamma^+\Gamma^- \qquad (4.42)$$

Now, comparing both sided of the equation (4.42), we get

$$\begin{bmatrix} \gamma_0 & 0 & 0 & 0 & \cdots & 0 & 0 \\ \gamma_2 & -\gamma_1 & \gamma_0 & 0 & \cdots & 0 & 0 \\ \gamma_4 & -\gamma_3 & \gamma_2 & -\gamma_1 & \cdots & 0 & 0 \\ \vdots & \vdots & \vdots & \vdots & \ddots & \vdots & \vdots \\ 0 & 0 & 0 & 0 & \cdots & (-1)^{m-1}\gamma_{m-1} & (-1)^m\gamma_{m-2} \\ 0 & 0 & 0 & 0 & \cdots & 0 & (-1)^m\gamma_m \end{bmatrix} \begin{bmatrix} C_{0,0} \\ C_{1,0} \\ C_{2,0} \\ \vdots \\ C_{(m-1),0} \\ 1 \end{bmatrix} =$$

$$\begin{bmatrix} \hat{p}_0 + {\gamma_0}^2 \\ \hat{p}_2 + 2\gamma_0\gamma_2 - {\gamma_1}^2 \\ \hat{p}_4 + \gamma_0\gamma_4 - 2\gamma_1\gamma_3 + {\gamma_2}^2 \\ \vdots \\ \hat{p}_{2(m-1)} + 2(-1)^m\gamma_m\gamma_{m-2} - (-1)^{(m-1)}\gamma_{m-1}^2 \\ (-1)^m + (-1)^m{\gamma_m}^2 \end{bmatrix} \qquad (4.43)$$

The coefficients of P_0 i.e. $C_{0,0}$, $C_{1,0}$, $C_{2,0}$, …, $C_{(m-1),0}$ can be obtained by solving equation ( ). Using these values, coefficients of P_1 i.e. $C_{0,1}$, $C_{1,1}$, $C_{2,1}$, …, $C_{(m-1),1}$ can be calculated from the following equation,

$$C_{i,1} = (-1)^i(C_{i,0} - \gamma_0) \qquad \text{with } i = 0, 1, \ldots, (m\text{-}1) \qquad (4.44)$$

Condition-2: $Q_0^+ = -Q_1^-$

From (4.36) we get,

$$\hat{L}(z) = Q_0^-(P_0^+ + P_1^-) \qquad (4.45)$$

Now, procedures shown for condition can be followed. But equation for obtaining coefficients of P_1 from coefficients of P_0 will change and become as follows,

$$C_{i,1} = (-1)^i(\gamma_0 - C_{i,0}) \qquad \text{with } i = 0, 1, \ldots, (m\text{-}1) \qquad (4.46)$$

4.3 Multi-Rate Control

Multi-rate control of sampled-data/discrete-time systems has continued to be a topic of interest since the late 1950's [42]. It is a control scheme where the plant output is sampled at a rate different than that at which its input is updated. The systems which use more than one sampling rate are called Multi-Rate digital control systems.

4.3.1 Types of multi-rate control:

Let T be the interval corresponding to the faster of the two sampling rates as mentioned in the definition. Then, In case of SISO plants, multi-rate control can be divided into two categories [17]:

- **Fast-Input Control:** Here the controller updates the plant input at a rate faster than the rate at which it samples the plant output. It may be denoted as (MT, T)-control.

- **Fast-Output Control:** Here the controller samples the plant output at a faster rate than the rate at which it updates the plant input. It may be denoted as (T, MT)-control.

Here, M=1 signifies LTI control and M = 2 signifies 2-rate control and so on.

4.3.2 Why multi-rate control?

For plants having unstable poles and NMP zeros an LTI controller may not yield sufficient gain margin(GM) and phase margin(PM) i.e. robust compensation cannot be achieved for such plants. Also pole-zero cancellation can not be used to remove the NMP zeros to avoid internal instability. So in this context attempts have been made to achieve zero placement using multi-rate control. It can be done better by using FAST-OUTPUT control in comparison to FAST-INPUT control [17].

4.3.3 Fast-Output Controller scheme:

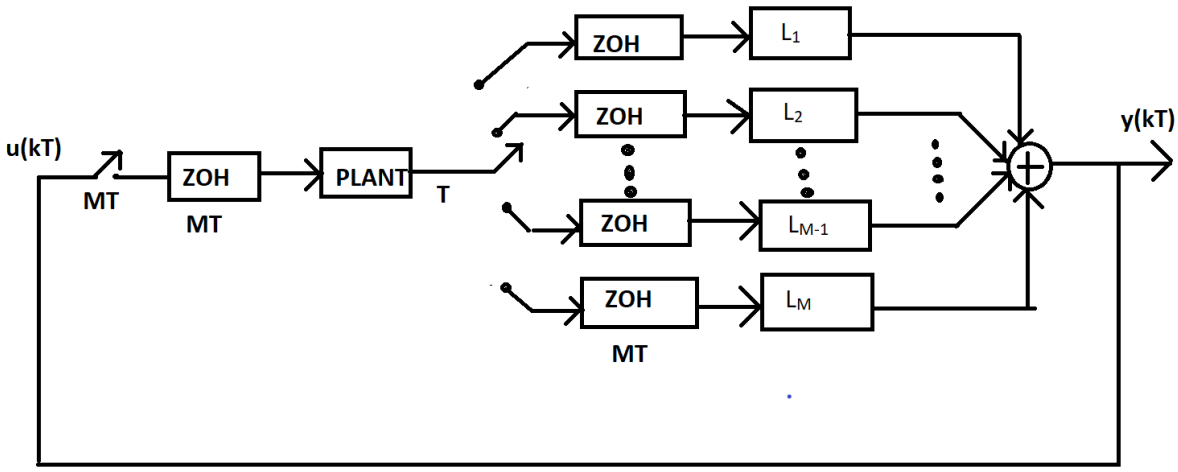

Fig.27: Fast-output controller scheme

In the fast-output control scheme, as shown in Fig-27, the plant output is detected at M uniformly spaced (T-interval) instants and based on these values the controller output is updated only once during the period MT and held constant at the same value during the subsequent (M −1) instants (at T-intervals).

It can be of two types:

- Even instant plant input updating
- Odd instant plant input updating

We can represent the above two cases in a general way as:

$$u(2N + i) = k_1 y(2N + i) + k_0 y(2N + i - 1) \quad (4.47)$$

$$u(2N + i + 1) = u(2N + i) \quad (4.48)$$

Where k_1 and k_0 are time-invariant gains, and i can be 0 or 1, which represents Even or Odd instant updating, respectively.

4.3.4 Fast-Input Controller scheme:

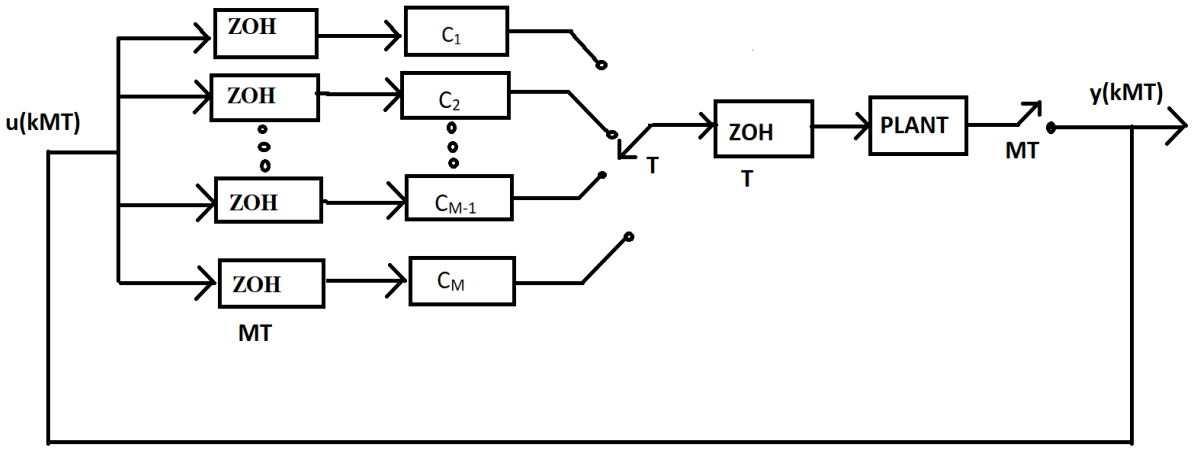

Fig.28: Fast-input controller scheme

In the fast-input control scheme, as shown in Fig-28, the plant output is detected at MT-intervals while the input is excited at T-intervals. Thus, the non-observance of $(M-1)$ out of the M numbers of plant outputs makes the system susceptible to being non-regulated for the non-observed instants.

It can also be of two types:

- Even instant plant input updating
- Odd instant plant input updating

Here also we can represent the above two cases in a general way as:

$$u(2N+i) = k_1 y(2N+i) \qquad (4.49)$$

$$u(2N+i+1) = k_0 y(2N+i) \qquad (4.50)$$

Where k_1 and k_0 are time-invariant gains, and i can be 0 or 1, which represents Even or Odd instant updating, respectively.

Some important points regarding fast input and fast output control:

1. From (MT, MT)-control i.e. LTI control point of view (MT, T)-control, i.e. Fast-Input Control, can effect zero placement and hence provides better robustness.
2. But the inter-sample behaviour of such systems are unacceptable. The T-interval responses of such systems contained large amount of swings/high oscillation.

3. Whereas for (T, MT)-control, i.e. Fast-Output Control, systems, the controller output remains intact for MT-intervals. So, they are not inherently susceptible to such inter-sample problems.
4. 2-rate control i.e. by taking M=2, we can describe 2-rate control from a 2-periodic perspective.
5. Generalized Multi-rate control can be considered as a Periodic control in augmentation with an LTI component.

4.4 Multi (2)-Rate Control from a 2-Periodic Perspective: Generalized 2-Rate Control

2-rate controllers using a 2-periodic perspective lead to the revelation that the fast-output 2-rate controllers can also effect zero placement and hence robust control with satisfactory response. In fact a generalized version of 2-rate controllers used so far has also been proposed in [17],[20] and the same is shown to be capable of handling third and higher order plants as well.

4.4.1 Block Diagram

The block diagram of a generalised m-th order 2-rate controller is shown in Fig. 29:

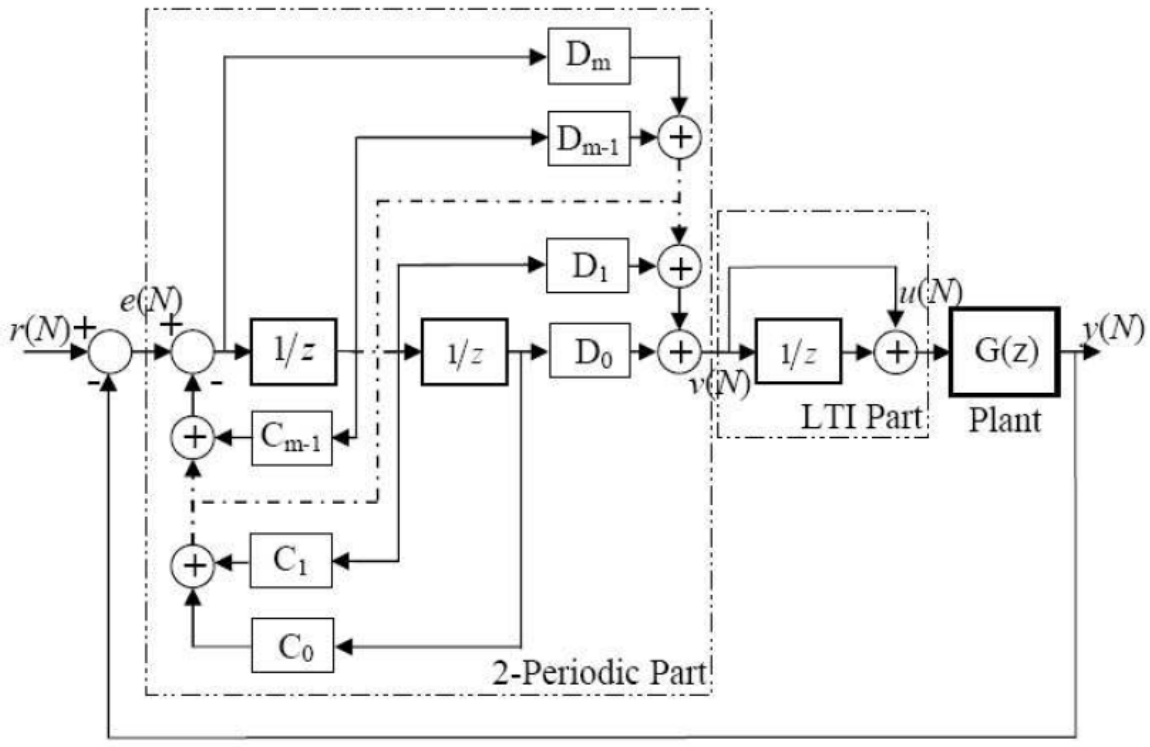

Fig-29: A Generalised m-th order 2-rate controller

By augmenting our plant with $\left(1+\frac{1}{z}\right)$ and then applying periodic control in it we can get benefits of both 2-rate and 2-periodic control.

4.4.2 Illustrative Example:

Let us consider a second order system consisting non-minimum phase

$$G(z) = \frac{(z-1.3)}{(z-0.5)(z-1.5)} \tag{4.51}$$

Augmenting the plant with $\left(1+\frac{1}{z}\right)$ we get:

$$G(z) = \frac{(z-1.3)(z+1)}{z(z-0.5)(z-1.5)} \tag{4.52}$$

By choosing the desired closed loop poles, controller poles and the loop-zero positions carefully then following ( ), the corresponding pole and zero polynomials become:

$$\widehat{\mathrm{A}}(\mathrm{z}^2) = -\mathrm{z}^2(\mathrm{z}^2-0.25)(\mathrm{z}^2-2.25), \widehat{\mathrm{P}}(\mathrm{z}^2) = \mathrm{z}^2(\mathrm{z}^2-0.322),$$

$$\tilde{\mathrm{Z}}(\mathrm{z}^2) = -0.872(\mathrm{z}^2)^3(\mathrm{z}^2-0.25), \breve{\Delta} = -(\mathrm{z}^2)^2(\mathrm{z}^2-0.25), \text{and } \widetilde{\mathrm{D}}(\mathrm{z}^2) = (\mathrm{z}^2-0.85)^2$$

Then applying the condition $\mathrm{Q}_0^+ = -\mathrm{Q}_1^-$ and $\hat{\mathrm{L}}(\mathrm{z}) = Q_0^-(P_0^+ + P_1^-)$ we get the controller parameters as:

$$d_{0,0} = d_{0,1} = 0, \quad d_{1,0} = d_{1,1} = 0, \quad d_{2,0} = -d_{2,1} = 5.08, \quad c_{0,0} = c_{0,1} = 0.2785,$$

$$and \quad c_{1,0} = 1.0794, c_{1,1} = -0.5348$$

By putting it in the below circuit shown, with initial condition given:

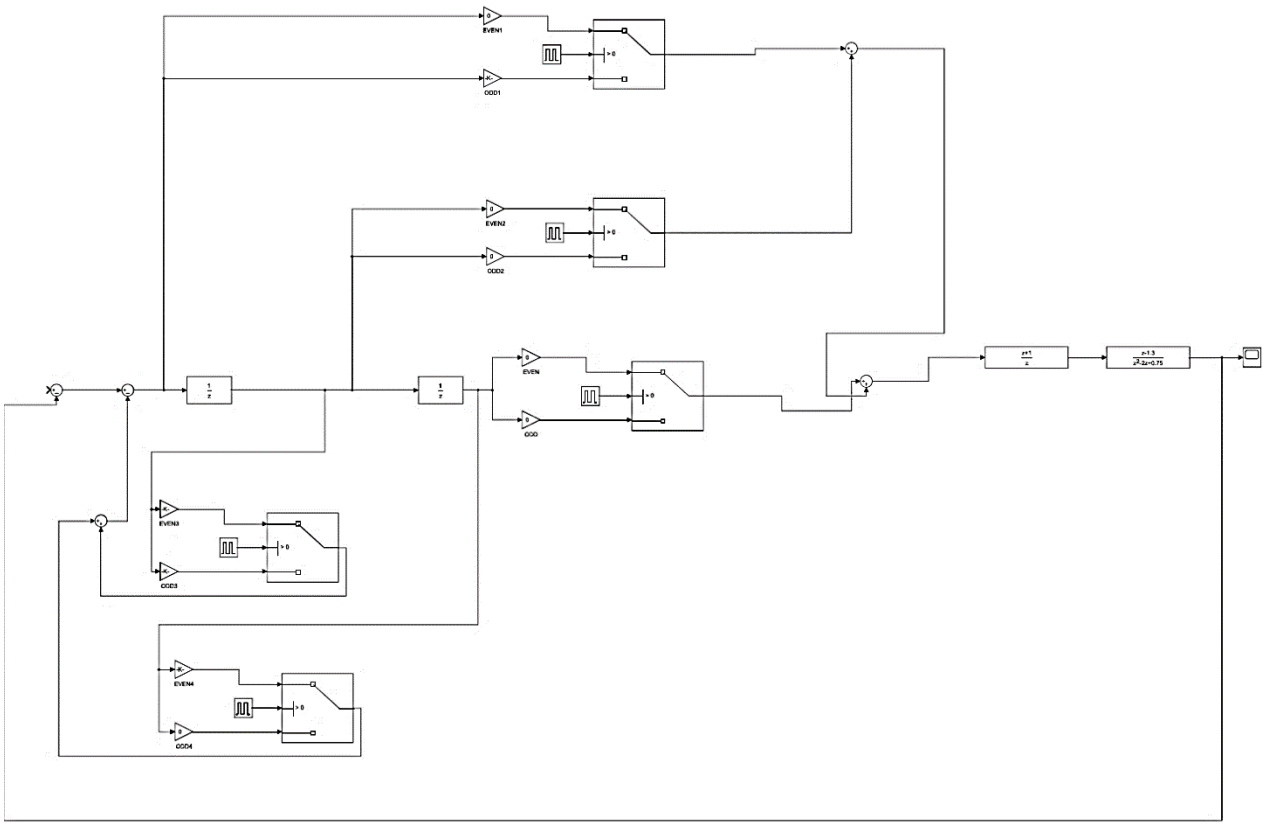

Fig.30: MATLAB Simulink implementation of 2-rate control

The zero-input response of the system is as shown in Fig. 31.

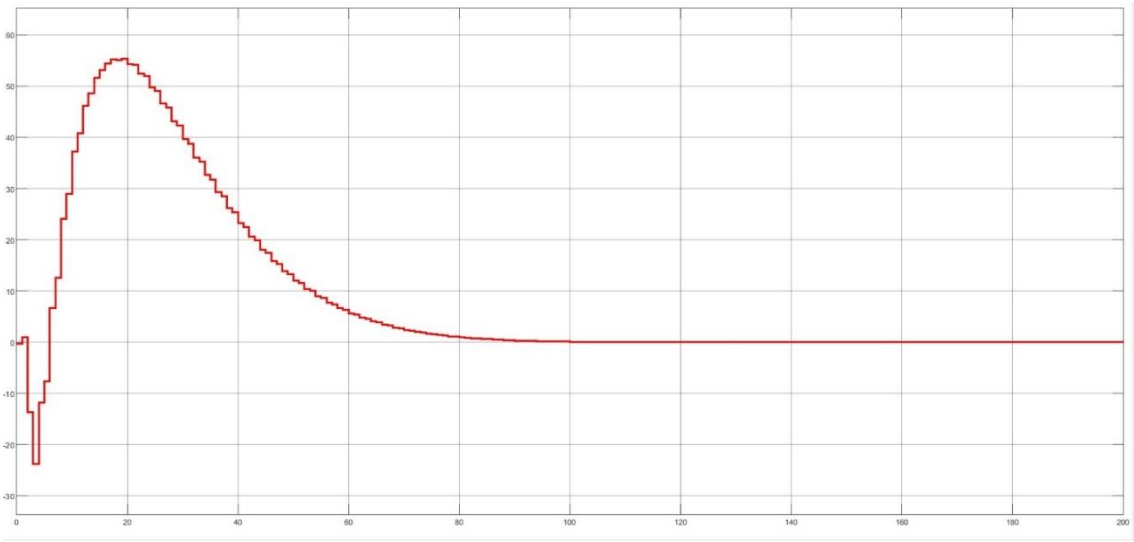

Fig.31: Output response curve of Fig.30 simulation

The root locus of the compensated system is as given in Fig. 32. As can be seen here the loop-zeros are relocated within the unit circle thus yielding a significantly better Gain Margin as compared to LDTI controllers. The GM value is 5.07.

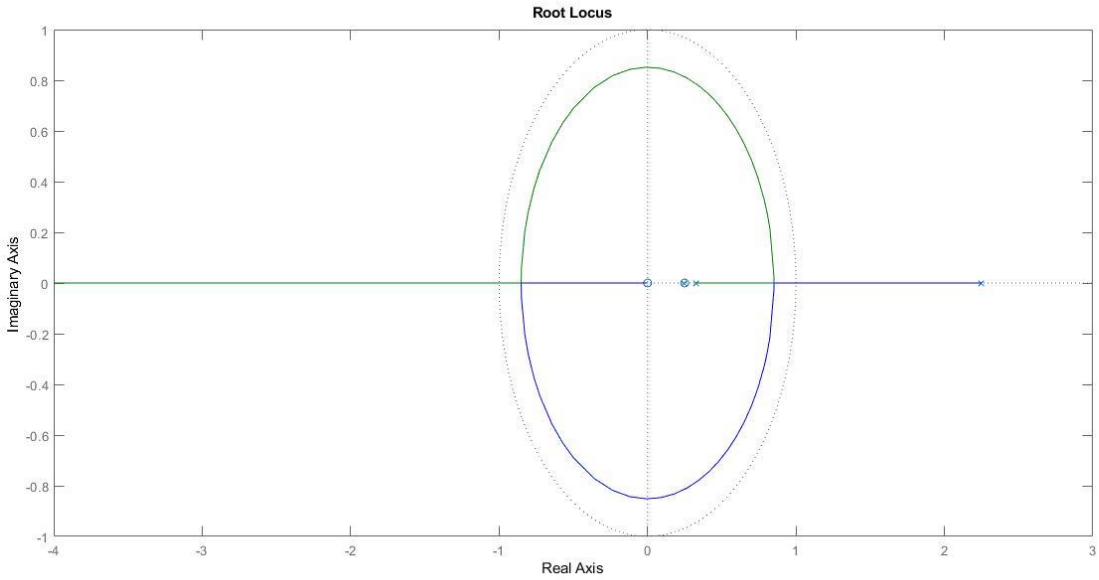

Fig.32: Root Locus of the system compensated by Multi (2)-rate control

Chapter 5

Implementation of 2-Rate Control for Boost Converter

5.1 Augmentation of boost converter

In Chapter 3 a double-loop PI control technique for the boost converter is discussed. However, in the closed inner loop transfer function, after compensating with PI-controller, there exists a non-minimum phase zero which is:

$$G_{in}(z) = \frac{C_1(z)G_1(z)}{1+C_1(z)G_1(z)} = \frac{2.2942(z-0.4258)}{(z+0.1681)(z+0.1281)} \tag{5.1}$$

The NMP zero can cause certain complications in the system specifically in terms of robustness margin. We already discussed about NMP pole and zero in Chapter 4. To overcome such a situation, we propose a multi (2)-rate control in the outer loop instead of PI-controller. So in the inner loop there is PI-control and in the outer loop there is Multi-Rate control.

In chapter 4 the realization of a generalized 2-rate control using a 2-periodic control and an LTI part was discussed. Similarly, here we will augment the plant with an LTI part $\left(1+\frac{1}{z}\right)$ which in conjunction with 2-periodic controller will form a multi-rate control.

Without augmentation the effective plant transfer function was:

$$G_{in}(z) * G_2 = \frac{-23.582(z-0.4258)(z-1.015)}{(z+0.1681)(z+0.1281)(z-0.9968)} \tag{5.2}$$

Following the augmentation, the transfer function becomes:

$$G_{out}(z) = \frac{-23.582(z-0.4258)(z-1.015)(z+1)}{z(z+0.1681)(z+0.1281)(z-0.9968)} \qquad (5.3)$$

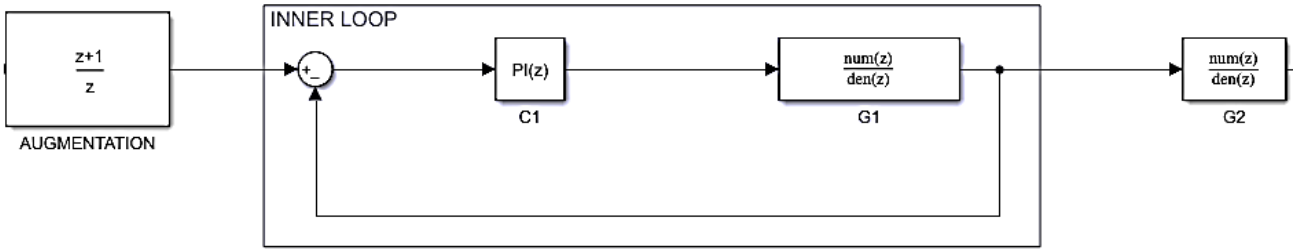

Fig.33: Augmentation Block Diagram

Now, we shall describe the steps to obtain the controller parameters to achieve arbitrary pole as well as loop-zero placement.

5.2 Controller Synthesis

In this section we shall discuss the steps involved in obtaining the controller gains.

A. Lifting the plant:

$$\hat{A}(z^2) = a^+a^- = z^2(z^2-0.9936)(z^2-0.0164)(z^2-0.02825) \qquad (5.4)$$

B. Order of the controller(m):

n=order of denominator of plant=4; *r*=order of numerator of plant=3

$$m = 4 - I^+\left(\frac{4-3}{2}\right) = 3 \qquad (5.5)$$

C. Choosing controller poles:

We are choosing the controller poles at origin to ensure that we can relocate loop zeros as well (if possible at origin) to improve loop robustness.

$$\hat{P}(z^2) = (-z^2)^3 \qquad (5.6)$$

D. Desired closed loop poles:

The order of the plant is 4; hence there must be 4 desired pole locations. As 3 controller poles are selected to improve stability of the plant, so 3 of the desired poles are placed at same location. Remaining one pole is chosen such that it is away from but inside the unit circle as

$$\breve{\Delta}(z^2) = z^6(z^2-0.02825) \qquad (5.7)$$

E. Additional closed-loop poles introduced by the controller:

Seeing Root Locus of the augmented plant the additional closed-loop poles are chosen.

$$\tilde{D}(z^2) = -z^2(-z^2 + 0.2)^2$$

F. Loop zero polynomial:

From eqn. (4.27) we got:

$$\hat{A}(z^2)\hat{P}(z^2) + k\tilde{Z}(z^2) = \hat{\Delta}(z^2) = \breve{\Delta}(z^2)\tilde{D}(z^2) = 0 \quad (5.8)$$

$$=> k\tilde{Z}(z^2) = \breve{\Delta}(z^2)\tilde{D}(z^2) - \hat{A}(z^2)\hat{P}(z^2) \quad (5.9)$$

Solving we get, $\tilde{Z}(z^2) = -0.61z^8[z^4 + 0.01061z^2 - (1.09 * 10^{-3})]$ (5.10)

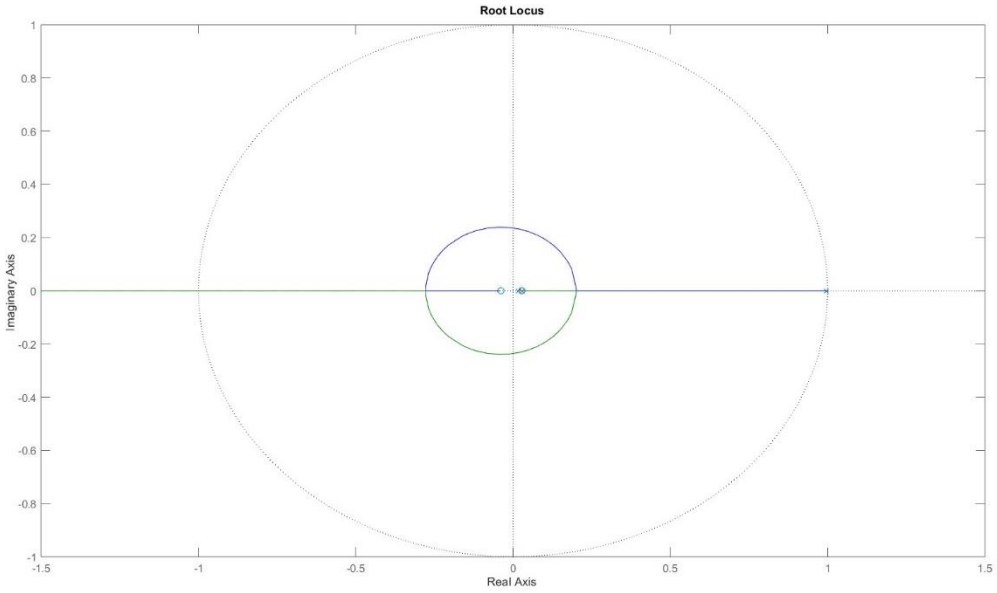

Fig.34: Root locus for 2-rate compensated plant

The root locus corresponding to the equivalent time-lifted loop transfer function is shown in Fig. 34. As can be obtained from the root locus the GM for the 2-rate compensated system will be 3.46, which can be shown to be significantly larger than the GM obtained by employing PI controller in the outer loop.

G. Order of the controller (θ):

From eqn. (4.27): $\theta = m + \eta \ with \ \eta = n - I^+\left\{\frac{n-r}{2}\right\} = 4 - 1 = 3$

Thus, $\theta = 3 + 3 = 6$ (5.11)

H. Controller Synthesis:

a) $\tilde{Z}(z^2) = r_0 + r_2z^2 + r_4z^4 + r_6z^6 + r_8z^8 + r_{10}z^{10} + r_{12}z^{12}$ as $\theta = 6$ (5.12)

b) Expanding eqn. (5.10) we get:

$$\tilde{Z}(z^2) = -0.61z^{12} - 0.006472z^{10} + 0.0006649z^8 \quad (5.13)$$

Comparing with the polynomial

$$r_0 = 0; r_2 = 0; r_4 = 0; r_6 = 0; r_8 = 0.0006649; r_{10} = -0.006472; r_{12} = -0.61$$

c) $\varphi_1 = I^-\left\{\frac{n+r}{2}\right\} = I^-\left(\frac{7}{2}\right) = 3 \quad and \;\; \varphi_2 = I^-\left\{\frac{n+r-1}{2}\right\} = 3$

Now, $a^+b^- = \hat{B}(z) = \hat{B}_e(z^2) + z\hat{B}_d(z^2)$

$= \widehat{b_0} + \hat{b}_2z^2 + \hat{b}_4z^4 + \hat{b}_6z^6 + z[\hat{b}_1 + \hat{b}_3z^2 + \hat{b}_5z^4 + \hat{b}_7z^6]$

$= 0 + 0.2188z + 3.3z^2 + 13.43z^3 + 3.121z^4 - 37.52z^5 - 6.127z^6 + 23.58z^7 \quad (5.14)$

Thus, $\widehat{b_0} = 0; \hat{b}_1 = 0.2188; \hat{b}_2 = 3.3; \hat{b}_3 = 13.43;\ \hat{b}_4 = 3.121;\ \hat{b}_5 = -37.52; \hat{b}_6 = -6.127;\ \hat{b}_7 = 23.58$

d) $\hat{L}(z) = \hat{L}_e(z^2) + z\hat{L}_d(z^2) = \widehat{l_0} + \hat{l}_2z^2 + \hat{l}_4z^4 + \hat{l}_6z^6 + z[\hat{l}_1 + \hat{l}_3z^2 + \hat{l}_5z^4]$ (5.15)

e) $\tilde{Z}(z^2) = 2\hat{B}_e(z^2)\hat{L}_e(z^2) + 2z^2\hat{B}_d(z^2)\hat{L}_d(z^2)$

$$= r_0 + r_2z^2 + r_4z^4 + r_6z^6 + r_8z^8 + r_{10}z^{10} + r_{12}z^{12} \quad (5.16)$$

Thus by (4.39) we get the Sylvester matrix as,

$$\begin{bmatrix} r_0 \\ r_2 \\ r_4 \\ r_6 \\ r_8 \\ r_{10} \\ r_{12} \end{bmatrix} = 2 * \begin{bmatrix} \hat{b}_0 & 0 & 0 & 0 & 0 & 0 & 0 \\ \hat{b}_2 & \hat{b}_0 & 0 & 0 & \hat{b}_1 & 0 & 0 \\ \hat{b}_4 & \hat{b}_2 & \hat{b}_0 & 0 & \hat{b}_3 & \hat{b}_1 & 0 \\ \hat{b}_6 & \hat{b}_4 & \hat{b}_2 & \hat{b}_0 & \hat{b}_5 & \hat{b}_3 & \hat{b}_1 \\ 0 & \hat{b}_6 & \hat{b}_4 & \hat{b}_2 & \hat{b}_7 & \hat{b}_5 & \hat{b}_3 \\ 0 & 0 & \hat{b}_6 & \hat{b}_4 & 0 & \hat{b}_7 & \hat{b}_5 \\ 0 & 0 & 0 & \hat{b}_6 & 0 & 0 & \hat{b}_7 \end{bmatrix} \begin{bmatrix} \widehat{l_0} \\ \widehat{l_2} \\ \widehat{l_4} \\ \widehat{l_6} \\ \widehat{l_1} \\ \widehat{l_3} \\ \widehat{l_5} \end{bmatrix} \quad (5.17)$$

$$\begin{bmatrix} 0 \\ 0 \\ 0 \\ 0 \\ 0.0006649 \\ -0.006472 \\ -0.61 \end{bmatrix} = 2 * \begin{bmatrix} 0 & 0 & 0 & 0 & 0 & 0 & 0 \\ 3.3 & 0 & 0 & 0 & 0.2188 & 0 & 0 \\ 3.121 & 3.3 & 0 & 0 & 13.43 & 0.2188 & 0 \\ -6.127 & 3.121 & 3.3 & 0 & -37.52 & 13.43 & 0.2188 \\ 0 & -6.127 & 3.121 & 3.3 & 23.58 & -37.52 & 13.43 \\ 0 & 0 & -6.127 & 3.121 & 0 & 23.58 & -37.52 \\ 0 & 0 & 0 & -6.127 & 0 & 0 & 23.58 \end{bmatrix} \begin{bmatrix} \widehat{l_0} \\ \widehat{l_2} \\ \widehat{l_4} \\ \widehat{l_6} \\ \widehat{l_1} \\ \widehat{l_3} \\ \widehat{l_5} \end{bmatrix}$$

(5.18)

Now, since one row of the matrix is zero, so are reducing the rank of the matrix by eliminating the 1st row of $\bar{B}$-matrix and 1st element of $\hat{r}$-matrix and hence $\hat{l}_0$ also =0. Thus the matrix becomes:

$$\begin{bmatrix} 0 \\ 0 \\ 0 \\ 0.0006649 \\ -0.006472 \\ -0.61 \end{bmatrix} = 2 * \begin{bmatrix} 3.3 & 0 & 0 & 0 & 0.2188 & 0 & 0 \\ 3.121 & 3.3 & 0 & 0 & 13.43 & 0.2188 & 0 \\ -6.127 & 3.121 & 3.3 & 0 & -37.52 & 13.43 & 0.2188 \\ 0 & -6.127 & 3.121 & 3.3 & 23.58 & -37.52 & 13.43 \\ 0 & 0 & -6.127 & 3.121 & 0 & 23.58 & -37.52 \\ 0 & 0 & 0 & -6.127 & 0 & 0 & 23.58 \end{bmatrix} \begin{bmatrix} \widehat{l_2} \\ \widehat{l_4} \\ \widehat{l_6} \\ \widehat{l_1} \\ \widehat{l_3} \\ \widehat{l_5} \end{bmatrix} \tag{5.19}$$

Solving the above matrix equation we get:

$$\widehat{l_1} = 0; \widehat{l_3} = -3.8561; \widehat{l_5} = -7.3872; \widehat{l_2} = 0.2557; \widehat{l_4} = 15.9410; \widehat{l_6} = -28.3802$$

I. Controller Parameters:

To find the controller parameters we choose the condition: $Q_0^+ = Q_1^-$

Then from (4.40) one gets, $\hat{L}(z) = Q_0^-(P_0^+ - P_1^-)$

Now according to the condition discussed before in chapter 4 we divide the $\hat{L}(z)$ polynomial into two parts:

$$\hat{L}(z) = 0.2557z^2 + 15.941z^4 - 28.302z^6 - 3.8561z^3 - 7.3872z^5 \tag{5.20}$$

$$= (-28.38z^3 - 15.79z^2 + 11.88z)(z^3 - 0.296z^2 + 0.02152z) \tag{5.21}$$

Assigning the non-monic part as Q_0^- and the monic part as $(P_0^+ - P_1^-)$

$$\therefore Q_0^- = (-28.38z^3 - 15.79z^2 + 11.88z) \tag{5.22}$$

$$and\ (P_0^+ - P_1^-) = (z^3 - 0.296z^2 + 0.02152z) \tag{5.23}$$

a) Calculation of D_0, D_1, D_2, D_3:

From (4.6) for m=3

$$Q_0(z) = Q_0^+ = [d_{3,0}z^3 + d_{2,0}z^2 + d_{1,0}z + d_{0,0}] \tag{5.24}$$

$$\therefore Q_0^- = \left[-d_{3,0}z^3 + d_{2,0}z^2 - d_{1,0}z + d_{0,0}\right] = (-28.38z^3 - 15.79z^2 + 11.88z) \tag{5.25}$$

Thus by comparing:

$$d_{3,0} = 28.38; d_{2,0} = -15.79; d_{1,0} = -11.88;\ d_{0,0} = 0$$

Now, according to condition: $Q_0^+ = Q_1^-$

$$=> \left[d_{3,0}z^3 + d_{2,0}z^2 + d_{1,0}z + d_{0,0}\right] = \left[-d_{3,1}z^3 + d_{2,1}z^2 - d_{1,1}z + d_{0,1}\right] \quad (5.26)$$

Thus by comparing:

$$d_{3,1} = -d_{3,0} = -28.38;\ d_{2,1} = d_{2,0} = -15.79;\ d_{1,1} = -d_{1,0} = 11.88;\ d_{0,1} = d_{0,0} = 0$$

According to eqn. (4.3)

- $D_0 = d_{0,0} + d_{0,1} = 0\ (Even) \quad and \quad d_{0,0} - d_{0,1} = 0\ (Odd)$
- $D_1 = d_{1,0} + d_{1,1} = 0\ (Even) \quad and \quad d_{1,0} - d_{1,1} = -23.76\ (odd)$
- $D_2 = d_{2,0} + d_{2,1} = -31.58\ (Even) \quad and \quad d_{2,0} - d_{2,1} = 0\ (Odd)$
- $D_3 = d_{3,0} + d_{3,1} = 0\ (Even) \quad and \quad d_{3,0} - d_{3,1} = 53.76\ (Odd)$

c) Calculation of C_0, C_1, C_2:

From eqn. (4.41) for m=3 : $(P_0^+ - P_1^-) = \Gamma(z) = \gamma_0 + \gamma_1 z + \gamma_2 z^2 + \gamma_3 z^3$

$$= (z^3 - 0.296z^2 + 0.02152z) \quad (5.27)$$

By comparing: $\gamma_0 = 0; \gamma_1 = 0.02152; \gamma_2 = -0.296; \gamma_3 = 1$

From (4.29) for m=3 : $\hat{P}(z^2) = \hat{p}_0 + \hat{p}_2 z^2 + \hat{p}_4 z^4 - z^6 = -z^6$ (5.28)

By comparing: $\hat{p}_0 = 0;\ \hat{p}_2 = 0; \hat{p}_4 = 0$

From (4.42) we got : $P_0^+\Gamma^- + P_0^-\Gamma^+ = \hat{P}(z^2) + \Gamma^+\Gamma^-$

Expressing the above equation in matrix form for m=3 we get:

$$2\begin{bmatrix} \gamma_0 & 0 & 0 & 0 \\ \gamma_2 & -\gamma_1 & \gamma_0 & 0 \\ 0 & -\gamma_3 & \gamma_2 & -\gamma_1 \\ 0 & 0 & 0 & -\gamma_3 \end{bmatrix}\begin{bmatrix} c_{0,0} \\ c_{1,0} \\ c_{2,0} \\ 1 \end{bmatrix} = \begin{bmatrix} \hat{p}_0 + \gamma_0^2 \\ \hat{p}_2 + 2\gamma_0\gamma_2 - \gamma_1^2 \\ \hat{p}_4 - 2\gamma_1\gamma_3 + \gamma_2^2 \\ -1 - \gamma_3^2 \end{bmatrix} \quad (5.29)$$

Putting the values in the above matrix equation we get:

$$2\begin{bmatrix} 0 & 0 & 0 & 0 \\ -0.296 & -0.02152 & 0 & 0 \\ 0 & -1 & -0.296 & -0.02152 \\ 0 & 0 & 0 & -1 \end{bmatrix}\begin{bmatrix} c_{0,0} \\ c_{1,0} \\ c_{2,0} \\ 1 \end{bmatrix} = \begin{bmatrix} 0 \\ -4.631 * 10^{-4} \\ 0.0444 \\ -2 \end{bmatrix} \quad (5.30)$$

Solving the above matrix equation we get: $c_{0,0} = 0.0037; c_{1,0} = -0.0402; c_{2,0} = -0.012$

Thus from eqn. (4.44):

$$c_{0,1} = c_{0,0} - \gamma_0 = c_{0,0} - 0 = 0.0037 \tag{5.31}$$

$$c_{1,1} = -(c_{1,0} - \gamma_1) = -(-0.0402 - 0.02152) = 0.06172 \tag{5.32}$$

$$c_{2,1} = c_{2,0} - \gamma_2 = -0.012 - (-0.296) = 0.284 \tag{5.33}$$

According to eqn. (4.4)

- $C_0 = c_{0,0} + c_{0,1} = 7.4 * 10^{-3}\ (Even) \quad and \quad c_{0,0} - c_{0,1} = 0\ (Odd)$
- $C_1 = c_{1,0} + c_{1,1} = 0.02152\ (Even) \quad and \quad c_{1,0} - c_{1,1} = -0.10192\ (odd)$
- $C_2 = c_{2,0} + c_{2,1} = 0.272\ (Even) \quad and \quad c_{2,0} - c_{2,1} = -0.296\ (Odd)$

The proposed double-loop control of the Boost Converter is realized using MATLAB Simulink, the Simulink Model is shown in Fig. 35.

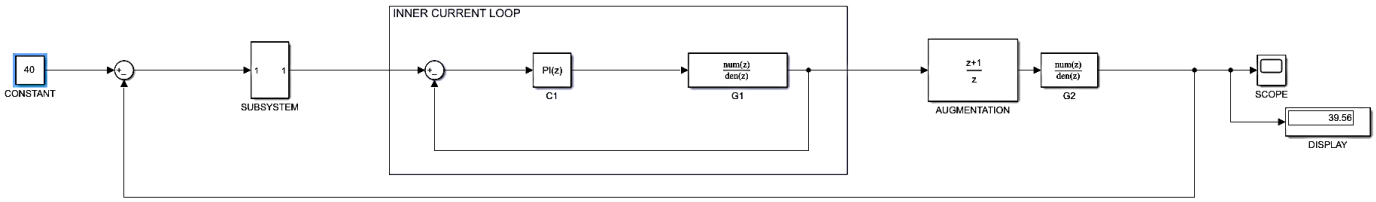

Fig.35: Double-loop control of boost converter with 2-rate control in outer loop

The simulation result for 2-rate compensated system is presented in Fig. 36.

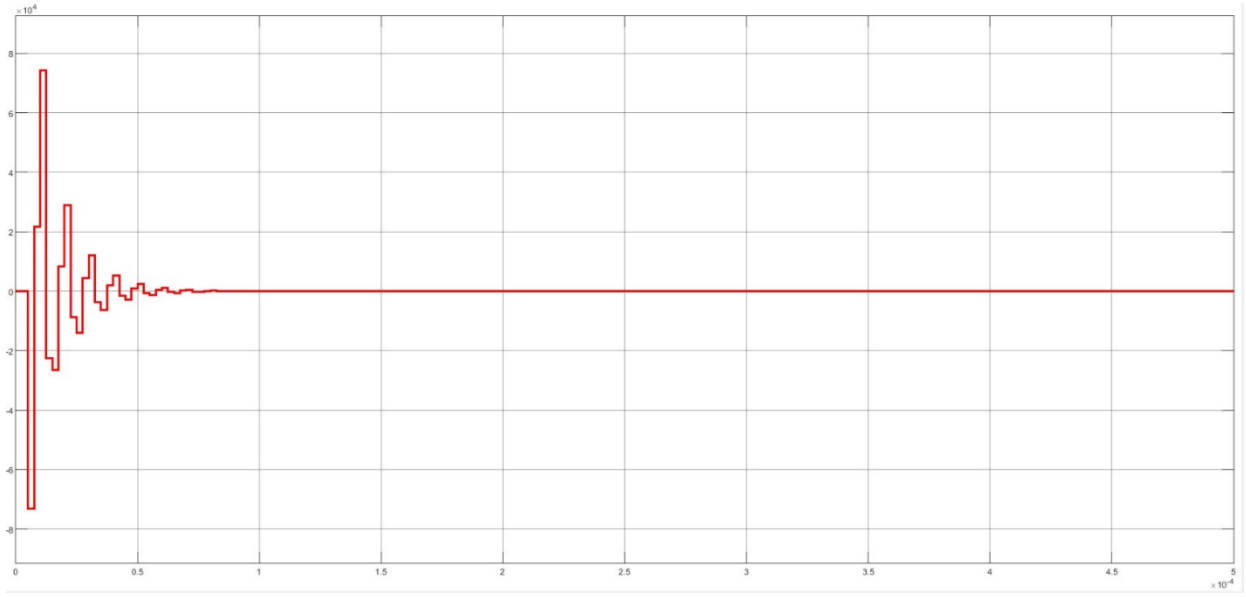

Fig.36: Output response curve for the 2-rate compensated system

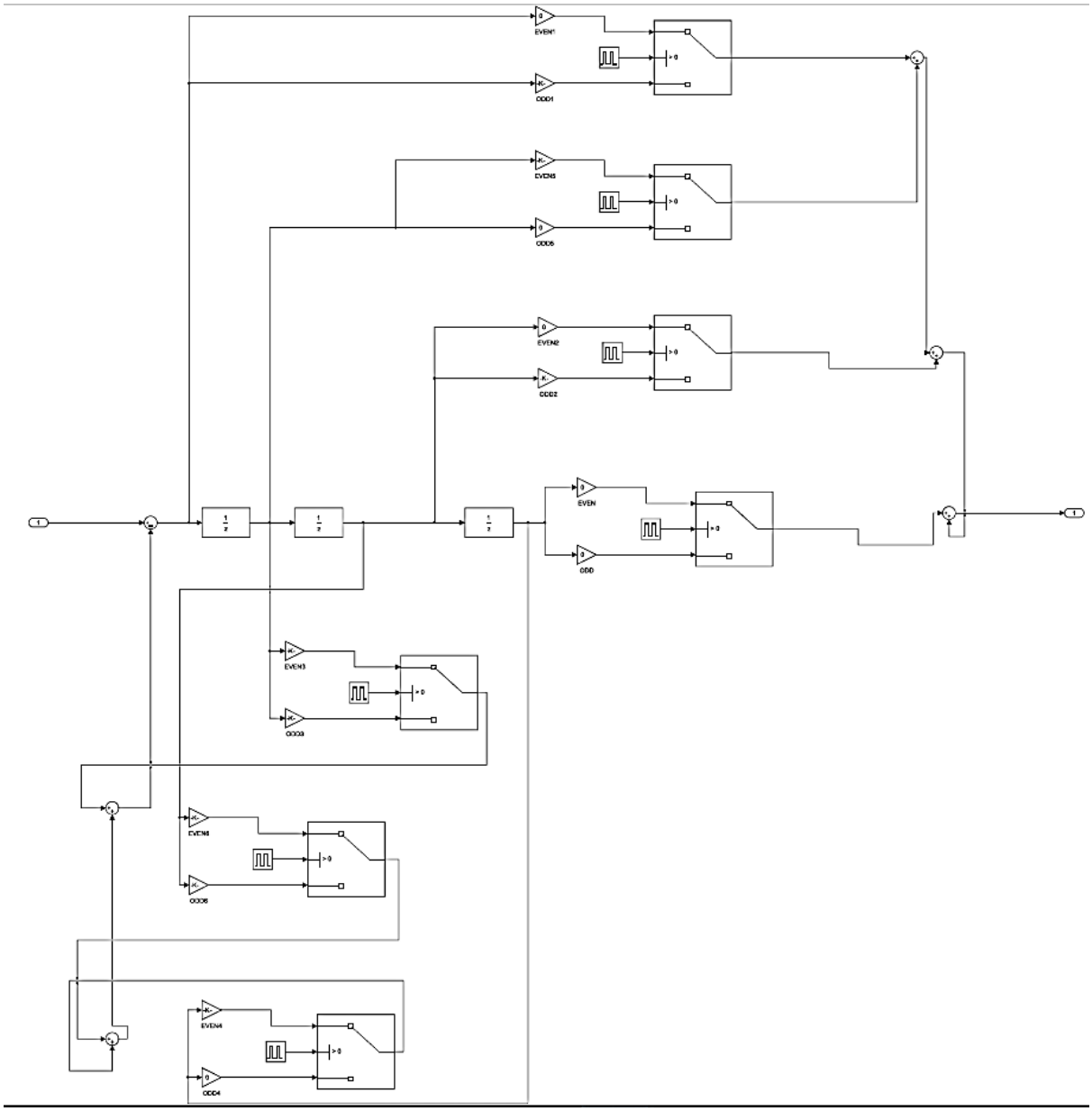

Fig.37: The subsystem model of 2-rate control shown in Fig.35

Finally, the proposed control topology, along with the Boost converter, is implemented for an Wind Power Generation System via MATLAB Simulink as shown in Fig. 38.

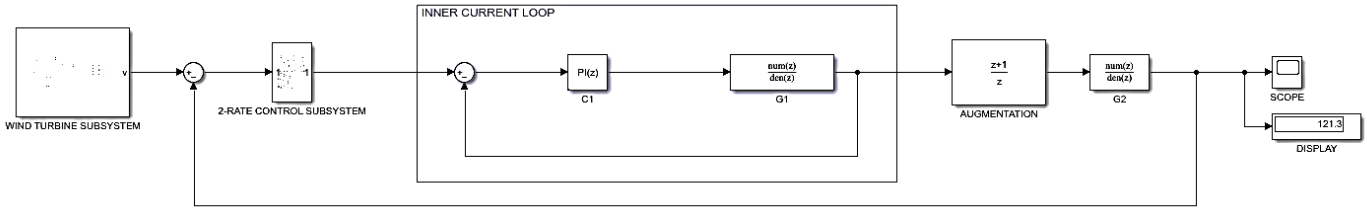

Fig.38: Simulink model of Wind turbine and boost converter with 2-rate compensation

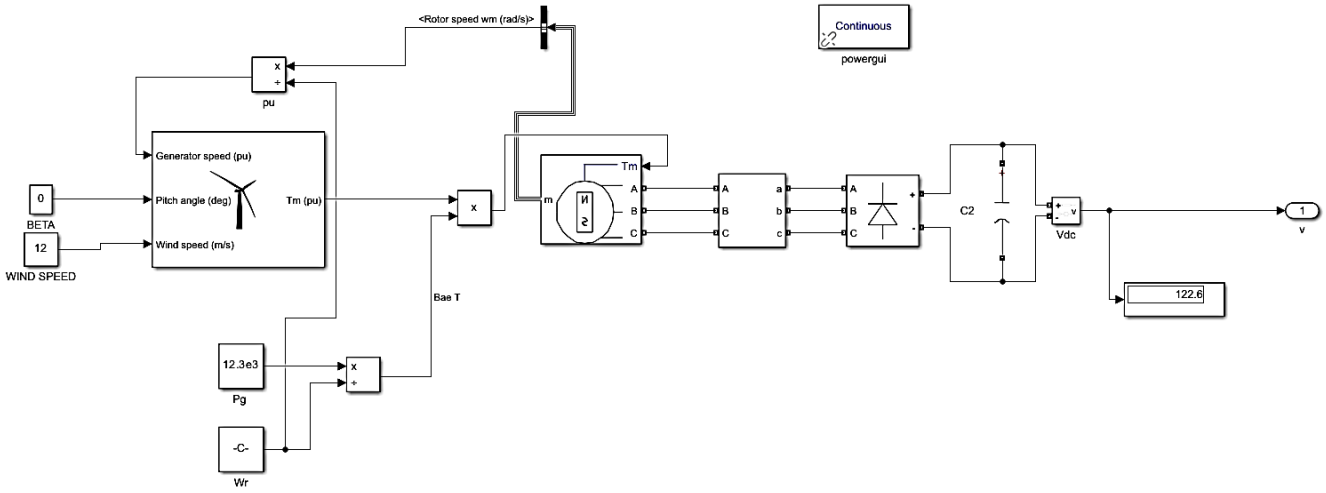

Fig.39: Wind Turbine Subsystem

The response for the proposed double-loop compensation of the Boost Converter for the simulated Wind Power Generation scheme is as shown in Fig. 40.

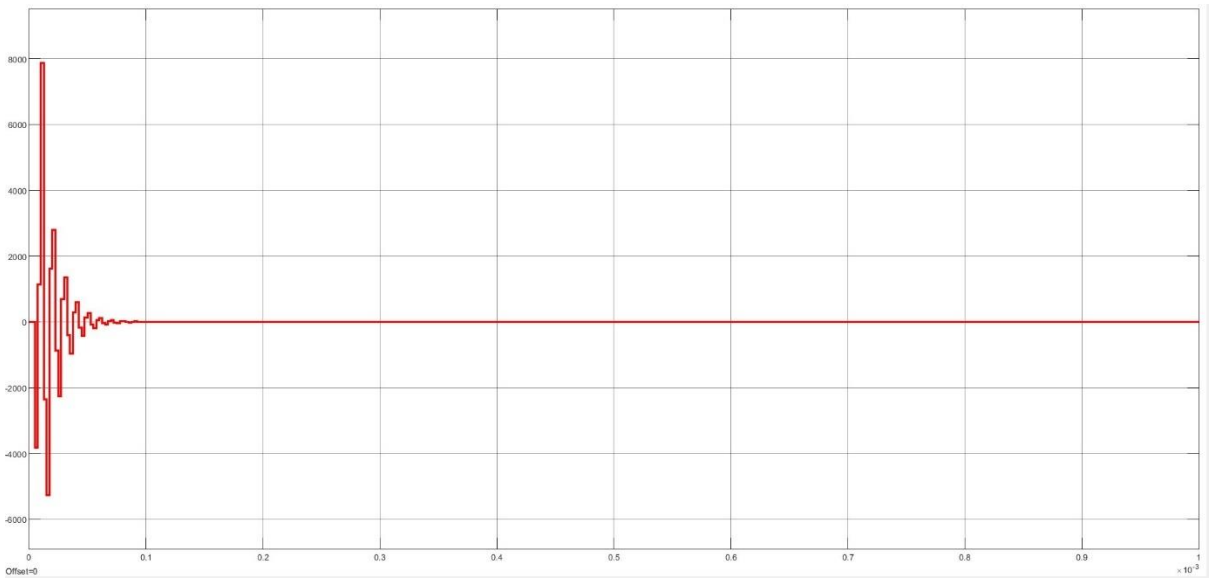

Fig.40: Output response curve for double-loop compensation of boost converter for wind power generation

5.3 Conclusions:

This chapter shows how the generalized 2-rate control can be realized as a combination of a 2-periodic controller along with an LTI part. A controller topology involving PI controller at the inner loop and a 2-rate controller at the outer loop is proposed and the methodology yields stable operation of the boost converter employed in wind generation applications. The simulation results are presented and it was found that the proposed 2-rate control scheme yields a better robustness margin as compared to double loop PI control scheme.

However, the transient behavior of the system response desires a lot of improvement. We intend to investigate further to improve the transient response so that it becomes acceptable.

Chapter 6

Conclusion and Future Scope

6.1 Conclusion

DC-DC boost converters are essential components in wind turbine systems, providing crucial functions such as voltage regulation, maximum power point tracking (MPPT), and power quality improvement. These converters ensure that the variable and often low-voltage output from wind turbines is efficiently stepped up to a stable level suitable for grid integration or storage. Despite the challenges posed by factors like the right-half-plane (RHP) zero, which affects control bandwidth and stability, boost converters have proven to be effective in enhancing the overall performance and reliability of wind energy systems.

The implementation of 2-rate controller for boost converters has enabled better robustness as compared to its LTI counterparts. Their role in stabilizing the power output is particularly critical for ensuring consistent and high-quality energy supply, which is essential for both standalone and grid-connected wind energy systems.

6.2 Future Scope

The future of DC-DC boost converters in wind turbine operations lies in overcoming the limitations and further optimizing their performance to meet the growing demands of renewable energy systems. Key areas of focus include:

1. **Improved Transient Behaviour:** A thorough investigation is needed to be carried out to modify the choice of controller and closed-loop poles to achieve acceptable transient response.

2. **Advanced Control Techniques**: Development of sophisticated control algorithms that can better handle the RHP zero and improve the dynamic response. This includes adaptive and predictive control strategies that can optimize performance under varying wind conditions.

3. **Integration with Energy Storage Systems**: Enhancing the role of boost converters in hybrid wind energy systems that include energy storage. This would involve developing converters that can efficiently manage bidirectional power flow, allowing for better storage and retrieval of energy in systems with batteries or other storage technologies.

4. **Improved MPPT Algorithms**: Advancing MPPT algorithms to be more responsive and accurate, particularly in rapidly changing wind conditions. Machine learning and AI-based algorithms could be explored to predict optimal operating points in real-time.

5. **Grid Support Functions**: Developing boost converters with enhanced grid support functionalities, such as reactive power compensation and frequency regulation, to help stabilize the grid and support the integration of higher levels of renewable energy.

6. **Integration with Smart Grids**: Investigating the role of boost converters in smart grid applications, where they could be used to dynamically manage power flows and contribute to grid resilience, especially as the penetration of wind energy continues to increase.

REFERENCES

[1] J. F. Manwell, J. G. McGowan, and A. L. Rogers, *Wind Energy Explained: Theory, Design, and Application*, 2nd ed., Hoboken, NJ, USA: Wiley, 2009.

[2] European Wind Energy Association (EWEA), *Wind Energy and the Environment*. Brussels, Belgium: EWEA, 2013.

[3] International Renewable Energy Agency (IRENA), *Renewable Energy Benefits: Leveraging Local Capacity for Onshore Wind*, Abu Dhabi, UAE: IRENA, 2017.

[4] Global Wind Energy Council (GWEC), *Global Wind Report 2020*. Brussels, Belgium: GWEC, 2020.

[5] T. Ackermann, *Wind Power in Power Systems*, 2nd ed., Hoboken, NJ, USA: Wiley, 2012.

[6] E. B. Arnett et al., *Impacts of Wind Energy Development on Wildlife and Wildlife Habitat*, Cham, Switzerland: Springer, 2016.

[7] T. Burton, D. Sharpe, N. Jenkins, and E. Bossanyi, *Wind Energy Handbook*, 2nd ed., Hoboken, NJ, USA: Wiley, 2011.

[8] E. Hau, *Wind Turbines: Fundamentals, Technologies, Application, Economics*, 3rd ed., Berlin, Germany: Springer, 2013.

[9] W. E. Leithead, "An Introduction to Wind Turbine Control," in *Springer Series on Energy*, Cham, Switzerland: Springer, 2007.

[10] W. Musial and B. Ram, *Large-Scale Offshore Wind Power in the United States: Assessment of Opportunities and Barriers*, Golden, CO, USA: National Renewable Energy Laboratory, 2010.

[11]Electrical4U, "Boost Converter (Step-Up Chopper)," *Electrical4U*. [Online]. Available: https://www.electrical4u.com/boost-converter-step-up-chopper/. [Accessed: Aug. 25, 2024].

[12] A. R. Ali and M. I. L. Saleh, *Renewable Energy Systems and Technologies*, 1st ed., Berlin, Germany: Springer, 2015.

[13] S. K. Jain and V. K. Gupta, "Performance Analysis of Boost Converter," *International Journal of Electronics and Electrical Engineering*, vol. 3, no. 2, pp. 143-150, Jun. 2011.

[14] S. H. Lee, "Advanced Control Techniques for Boost Converters," *IEEE Transactions on Power Electronics*, vol. 25, no. 6, pp. 1520-1530, Jun. 2010.

[15] M. W. O'Neill, *Practical Power Electronics*, 2nd ed., New York, NY, USA: Wiley, 2018.

[16] J. B. Miller, "Design Considerations for High Efficiency Boost Converters," *IEEE Power Electronics Conference*, pp. 152-159, Aug. 2014.

[17] S. Chakraborty, "2-periodic/2-rate compensation of discrete-time plants", Ph.D. dissertation, Indian Institute of Technology, Kharagpur, India, 2015.

[18] J. Dey, "Periodic compensation of continuous-time plants," Ph.D. dissertation, Indian Institute of Technology, Kharagpur, India, 2006.

[19] S. K. Das and S. Chakraborty, "Robust Compensation of Discrete-time Plant using 2-Periodic Controller," *7th IFAC Symposium on Robust Control Design*, *ROCOND 2012*, Alborg, Denmark, June 20-22, 2012.

[20] S. Chakraborty and S. K. Das, "Multi(2)-Rate Control From a 2-Periodic Perspective: Generalized 2-Rate Control", *IEEE Trans. Automatic Control,* Vol. 61, No. 6, pp. 1631 - 1636, 2016.

[21] S. K. Das and J. Dey, "Periodic Compensation of Continuous-Time Plants", *IEEE Trans. on Automatic Control,* Vol. 52, No. 5, pp. 898-904, May 2007.

[22] S. K. Das and P. K. Rajagopalan, "Techniques of analysis and robust control via zero placement of periodically compensated discrete-time plant" in *Control and Dynamics Systems, Advances in Theory and Applications*: Academic, Vol.74,1996.

[23] B. Kuo and F. Golnaraghi, *Automatic Control Systems*, 8th ed. New Delhi: Wiley India (P.) Ltd., 2012.

[24] Nirmal Murmu, "2-Periodic compensation of SISO discrete-time LTI plants", M. E. dissertation, Jadavpur University, India, 2017.

[25] A. W. Manyonge, et al., "Mathematical Modelling of Wind Turbine in a Wind Energy Conversion System: Power Coefficient Analysis," *Applied Mathematical Sciences*, vol. 6, no. 91, pp. 4527-4536, 2012.

[26] "Wind Energy Basics," American Wind Energy Association, [Online]. Available: https://www.awea.org/. [Accessed: Aug. 29, 2024].

[27] "Wind turbine parts and functions," Electrical Academia, [Online]. Available: https://electricalacademia.com/renewable-energy/wind-turbine-parts-functions/.[Accessed: Aug. 29, 2024].

[28] "What are Vertical Axis Wind Turbines?," ArborWind, [Online]. Available: https://blog.arborwind.com/what-are-vertical-axis-wind-turbines. [Accessed: Aug. 29, 2024].

[29] U.S. Department of Energy, [Online]. Available: https://www.energy.gov/. [Accessed: Aug. 29, 2024].

[30]"Wind turbine components," ResearchGate, [Online]. Available: https://www.researchgate.net/publication/322761950/figure/fig1/AS:631599280427055@1527596411910/Wind-turbine-components-1.png. [Accessed: Aug. 29, 2024].

[31] Kalyan Das, "Application of 2-periodic controller in boost converter for solar module", M. E. dissertation, Jadavpur University, India, 2019.

[32] National Programme on Technology Enhanced Learning (NPTEL). 'Control and Tuning Methods in Switched Mode Power Converters' NPTEL. Available: https://archive.nptel.ac.in/courses/108/105/108105180/. [Accessed: 29-Aug-2024]

[33] Z. Chen, W. Gao, J. Hu, and X. Ye, "Closed-loop Analysis and Cascade Control of a Nonminimum Phase Boost Converter", *IEEE Transactions on Power Electronics,* vol. 26, no. 4, pp.1237-1248, Apr. 2011.

[34] A. Ozdemir and Z. Erdem, "Double-loop PI controller design of the DC-DC boost converter with a proposed approach for calculation of the controller parameters," in *Proceedings of the Institution of Mechanical Engineers part I journal of Systems and Control Engineering*, 2017.

[35] F. Blaabjerg and K. Ma, "Future on Power Electronics for Wind Turbine Systems*," IEEE Journal of Emerging and Selected Topics in Power Electronics*, Vol. 1, no. 3, pp. 139-152, Sept. 2013.

[36] S. Heier, *Grid Integration of Wind Energy: Onshore and Offshore Conversion Systems*, 3rd ed. Wiley, 2014.

[37] M. Rashid, *Power Electronics: Circuits, Devices, and Applications*, 4th ed. Pearson, 2013.

[38] A. K. Jain and A. K. Agarwal, "A Comparative Study of Different Control Strategies for DC-DC Converters," in *Proceedings of the 2012 IEEE International Conference on Power Electronics, Drives and Energy Systems (PEDES),* Bengaluru, India, Dec. 2012.

[39] A. G. Yepes, F. D. Freijedo, Ó. López, and J. Doval-Gandoy, "High-Performance Digital Control for Single-Phase Active Power Filters Based on FPGA Implementation," *IEEE Transactions on Industrial Electronics*, Vol. 55, no. 8, pp. 2761-2770, Aug. 2008.

[40] Spandita Das, "2-Periodic Compensation of Discrete Time Plants: A 2-Degrees-of-Freedom Approach", M. E. dissertation, Jadavpur University, India, 2018.

[41] S.K. Das and P.K. Rajagopalan, "Periodic discrete-time system: stability analysis and robust control using zero placement", *IEEE Trans. Automatic Control*, Vol.37, pp. 374-378, Mar. 1992.

[42] G. Kranc, "Input-output analysis of multirate feedback systems", *IRE Trans. Automatic Control,* Vol. AC-3, pp. 21-28, Nov.1957.